A Wide Field CCD Survey for Low Surface Brightness Galaxies:

I. Data Acquisition, Description and Initial Results

Karen O'Neil and G.D. Bothun
Dept. of Physics, University of Oregon, Eugene OR, 97403

email:karen@moo.uoregon.edu

email:nuts@moo2.uoregon.edu

and

Mark E. Cornell
McDonald Observatory, University of Texas, Austin TX, 78712

email:cornell@puck.as.utexas.edu

Received ______________________; accepted ______________________

ABSTRACT

A Low Surface Brightness (LSB) galaxy survey of the Cancer and Pegasus galaxy clusters, and the low density regime defined by the Great Wall, was undertaken between 14 October 1993 and 17 April 1996 using the University of Texas MacDonald Observatory 0.8m telescope and a Loral-Fairchild 2048x2048 CCD camera. 127 galaxies were found with $\mu_B(0) \geq 22.0$ mag/arcsec^2, 119 of which are previously unidentified. Structural parameters ($\mu_{\rm B}(0)$, α, r_{25}, etc) and colors (using Johnson/Cousins U,B,V,I, & R filters, when possible) were determined for the galaxies. The majority of these galaxies (80%) were well fit by an exponential profile, while the remaining were either fit by a king profile (17%) or were too clumpy to be fit by any curve (3%). None of the galaxies were fit by a de Vaucouleurs (1959) $r^{1/4}$-type profile. The average central surface brightness of the sample is 23.06±0.20 mag/arcsec^2. The central surface brightness distribution of the galaxies is flat from 22.0 $\mu_B(0)$ to 24.0 $\mu_B(0)$, at which point a sharp drop-off is observed. By eliminating the possibility the drop-off is due to selection or distance effects, we show that it is highly likely the drop-off is due to the inability for extremely LSB galaxies to form in the cluster environment. Finally, previous data has shown that LSBs are deficient in molecular gas and dust. If we assume that LSBs have no dust and correct the sample to face-on surface brightness, the lowest surface brightness disk we detected has $\mu_B(0) = 27.1$. However, this sample shows the same non-correlation between inclination and central surface brightness that is seen for the case of high surface brightness galaxies. This non-correlation has been used as an argument to support the notion that disk galaxies are optically thick. Since its extremely unlikely that LSBs are optically thick (i.e. none are IRAS sources) this non-correlation most likely reflects the large intrinsic range of disk galaxy surface brightness instead of variations in disk galaxy opacity.

Subject headings: galaxies: low surface brightness

1. Introduction

Targeted searches for low surface brightness (LSB) galaxies have been ongoing for the past decade. This 10 year discovery effort has culminated with the result that LSB galaxies appear to constitute at least 50% of the general galaxy population (see McGaugh et al 1995a, McGaugh 1996). That we could actually have missed such a large component to date clearly shows that previous surveys have been strongly biased against detecting LSBs. Furthermore, as Sprayberry et al (1996) emphasize, LSB galaxies provide important corrections to the galaxy luminosity function and can account for much of the 'missing' baryonic mass in the Universe. As the study of the properties of LSB galaxies intensifies, (*e. g.* van der Hulst et al 1993, Bothun et al 1993, de Blok et al 1995, de Blok et al 1996, Dalcanton et al 1996), new insights into galaxy formation and evolution have resulted with the important implication that LSB galaxies might evolve in a fundamentally different manner than the process which has produced the Hubble Sequence (see Impey & Bothun 1997).

Previous surveys for LSB galaxies (*i. e.* Romanishin et al 1983, Schombert et al 1992, Impey et al 1996) have been photographically based. In general, those surveys have an isophotal limit for LSB detection that corresponds to a central surface brightness ($\mu_B(0)$) of 24.5–25.0 mag arcsec^{-2} . Other techniques such as photographic amplification (Malin 1978) and Tech Pan films (Schwartzenberg, et al 1996) have limits of 25.5 $\mu_B(0)$ - 26.5 $\mu_B(0)$. The very deep surveys of Virgo and Fornax by Impey et al 1988 and Bothun et al 1991, have a detection threshold of $\mu_B(0) = 27.0$ mag arcsec^{-2} . As this deeper survey was targeted, we cannot be confident that a 'representative' sample of LSB galaxies, defined as that which adequately samples the intrinsic distribution of $\mu_B(0)$, has been obtained. Thus, although we have had glimpses into the stellar population of LSB galaxies (*e. g.*

McGaugh & Bothun 1994), we do not have a complete picture of LSB galaxies' evolutionary processes. To improve upon these previous efforts, requires a sensitive CCD survey for LSB galaxies. Certainly the Sloan Digital Sky Survey (SDSS) promises to return a lot of LSB galaxies, but their secure detection requires good image recognition software as well as follow-up deeper CCD observations. As a precursor to the SDSS, we have used the 0.8-m telescope at McDonald Observatory and a 2048x2048 prime focus CCD camera (described in Claver 1995) to survey regions both in and outside of known clusters for galaxies with $22.0 \leq \mu_B(0) \leq 26.5$.

In this paper we describe the data acquisition and reduction process as well as the structural and morphological properties of this new sample of LSB galaxies. Paper II of this series (O'Neil, et al 1996, OBCI from now on) fully describes the multi-color data. In section 2 we describe the sky areas examined and instruments used to obtain the data. Section 3 gives the methods used to detect LSB galaxies while section 4 gives the techniques used to reduce and analyze the imaging data. Section 5 provides the structural properties of the sample, and section 6 describes the distribution of $\mu_B(0)$. Section 7 describes some of our more unusual surface brightness profiles. Finally, section 8 discusses the other structural properties of our sample as they relate to the opacity and morphology of LSB galaxies. All distance derived quantities are based on a distance scale using H_o = 100 km sec^{-1} Mpc s^{-1} and an infall velocity to Virgo of 300 km sec^{-1} .

2. Observations and Image Reduction

Over 5 separate observing runs between October 1993 and April 1996 UBVI images were acquired in a number of fields. The total sky surveyed was $\sim$27 degrees^2. Once identified, we determined the structural parameters ($\mu_B(0)$, α, r_{25}, etc.) and colors (from

Johnson/Cousins U,B,V,I, & R filters, when possible) for the 129 LSB galaxies discovered in these fields. In the blue, surface photometry in which errors on the individual isophotes are $\leq$ 0.25 mag was possible down to B $\sim$28.5 mag arcsec^{-2} . This is equivalent to a detection threshold in $\mu_B(0)$ of $\sim$27.0 mag arcsec^{-2} .

The data were acquired with the University of Texas McDonald Observatory 0.8m telescope between 14 October 1993 and 17 April 1996. A Loran-Farichild 2048x2048 pixel CCD camera was used with a 1.32" pixel size. The data sets consists of five consecutive nights of observing and then a separation of six months, repeated for a total of five data sets, We imaged a total of 25 degrees^2 of sky in at least three filters and another 2 degrees^2 in two filters. The journal of observations is summarized in Table 1.

Half the observed fields covered the Pegasus and Cancer clusters of galaxies (described in Bothun et al 1982). The remaining fields were centered around various (known) galaxies (table 1). The fields were chosen both because HSB galaxy surveys had already been done in those sky regions (giving us a reliable database of HSB galaxies for a comparison with our results) and to provide us with a complete (to 26.0$\mu_B(0)$) galaxy sample in both cluster and non-cluster environments. Much of this non-cluster environment is located in the Great Wall of galaxies first identified by Geller & Huchra (1989) and more fully characterized by Dell'Antonio et al (1996).

Six to eight (dome) flat field images were taken each night for each filter and were median combined to obtain the final field images for the night's data. The U, B, V, I and R flat field exposure times were 40s-70s, 3s-6s, 5s-20s, 0.4s-1.5s and 1s, respectively. Eight - ten Bias images were also taken for each observation run, with an exposure time of 0.01s. Dark field images were taken during the first data run (exp. time of 900s), but the dark current contribution to the overall noise was deemed insignificant (<0.1% contribution).

Johnson U,B and Kron-Cousins I filters were used for the 14-19 October 1993, 7-12 March 1994, 29 October - 3 November 1995, and 12-14 March 1996 data runs (runs 1,2,3, & 5 respectively). The U filter was also used during the 26-30 October 1995 run (run 4). A Johnson V filter was used during runs 1,4 and 5, and a Kron-Cousins R filter was used during run 4. The image quality through the I filter was particularly poor on the night of 9-10 March 1994 and those images were discarded. Typically, three images were taken through both the B (exp. time 600s) and U (exp. time 900s) filters, and one was taken in V (300s), I (120s), and R (180s). (Multiple images were offset to facilitate cosmic ray rejection.) To achieve the science goals of this survey, observing conditions had to be photometric to $\sim$5%. Thus we could tolerate some thin cirrus during the observations and many of the nights were noted as having such conditions.

Image processing was reluctantly done within the IRAF environment. First, all the images were inspected for obvious flaws such as filter ghosts or reflections. If any large flaws existed in the frame and an alternate frame in the same color was available, that frame was tossed. The flat and bias fields were also inspected visually and (median) combined to eliminate extraneous noise. The images were then bias subtracted and flat fielded using the standard IRAF IMARITH procedures. Multiple images of a field in the same color were shifted and registered and then averaged (median) using IRAF's IMCOMBINE routine to eliminate cosmic rays and other small scale flaws. The resultant images were then checked by eye to insure any registration errors were under 0.5 a pixel (0.66 ").

3. Galaxy Identification

Within the IRAF environment, each processed image was enlarged by a factor of four and scanned by eye for non stellar objects. By examining each processed image available in each field a minimum of two times, a list was compiled of all possible non stellar objects in every field which had a minimum radius of roughly 10 pixels (13.5"). Figure 1 shows the distribution of radii for our chosen galaxy sample. Every selected object was enlarged and examined in all available colors. After examination, any object proving not to be a galaxy (double stars, filter ghosts- which were a particular problem with these data, etc.) was discarded. The remaining objects then had their appearance checked against their image in one of the uncombined, unfiltered frames to insure no errors had occurred during the image processing phase (*e. g.* image registration errors, flat-field errors, etc). All of the remaining error-free objects with a reasonably low (apparent) central surface brightness ($\geq$22.0 $\mu_B(0)$ or $\geq$21.5 $\mu_V(0)$) were considered potential low surface brightness (LSB) galaxies and analyzed as such.

LSB galaxies often have a clumpy, non-spherical appearance and the fainter the galaxy, the higher the tendency toward an amorphous shape. If a galaxy is bright enough, automatic scanning methods such as the Automatic Plate Measuring system (APM) or FOCUS will usually identify the objects as non-stellar regardless of appearance. As the galaxies become fainter, however, automatic scanning systems rely on the galaxies having a core with contiguous pixels brighter than some threshold value and often will miss the more interesting LSB galaxies (e.g. P2-4). Thus, although our 'by eye' method of searching for LSB galaxies is more tedious than the the usual automatic scanning method, the non-conventional appearance of the very LSB galaxies makes our method more accurate in detecting all the objects to a central surface brightness of approximately 26.5 μ_B (1.0 – 2% of the sky brightness), giving us a more complete list of galaxies in the studied region than otherwise would be possible.

To check the accuracy of our search method (that is, to insure we were neither misidentifying galaxies as stars nor spurious objects as galaxies) a list of known HSB galaxies with $\mu_B(0) \geq 22.0$, $r_{27} \geq 7.0$" (obtained using the NED/IPAC extragalactic database, NED) in each field was checked against our list of each field's galaxies. When compared the lists matched to within 6% - 14 galaxies identified by NED were not among our eyeball detections and 15 were either supernovae, CCD flaws, or double stars misidentified (by us) as galaxies. Our list of LSB galaxies can thus be considered accurate (to $\mu_B(0) \leq 27.0$, $r_{27} \geq 7.0$") within an error of 6%. (The misidentification of supernovae and double stars as galaxies is probably less frequent in the LSB galaxy survey than in the HSB galaxy survey. Thus any errors in our LSB survey are more likely to result in our underestimating the total number of LSB galaxies in the surveyed regions.)

The search method - compiling separate lists of the galaxies for the different images of the same field - enabled us to examine the possibility of selection effects on galaxy identification for the different color images. All LSB galaxies were independently found in the B, V and R filters (when available). Frequently, galaxies were not originally identified in the U and I filters and were found only after being identified in the brighter (B and/or V) fields. Occasionally , extremely LSB objects were never detected in the U and I filters. Because each field had at least one image in V or B, color selection effects probably did not affect the results of our survey, nor would it affect any similar survey which included a broadband filter in the B, V, or R range.

4. Data Analysis

Zeropoints were found for each field by identifying known galaxies (Bothun, et al 1985, Zwicky 1961) and standard stars (Landolt 1973,1983) within the fields. The colors for the known galaxies were compared to the (sky-subtracted) colors obtained through IRAF's QPHOT procedure, and a zeropoint was obtained. The zeropoints (3–6 for each field/filter) were averaged and used for all the images from that field that night. If insufficient information was found to obtain a field's zeropoint in this way (not enough reference galaxies/stars were identified in the field), its zeropoint was obtained from nearby fields observed the same night. The r.m.s. scatter between the zeropoints was typically 1–2%. (See OBCI.)

The peak intensity was found for each LSB galaxy and ellipses were fit around that point to obtain the intensity in each annulus using the GASP software package (Cawson 1983). In the cases where no obvious peak intensity existed in the galaxy (the clumpier LSB galaxies) the physical center, estimated by centroiding with respect to the our isophotes, of the galaxy was chosen. Because of the coarse pixel size of many of the galaxies in this survey, our accuracy in locating galactic centers was only good to within 2". Surface brightness profiles and other data cannot be trusted inside that boundary, which also corresponds well with the typical size of the seeing disk. The average sky-subtracted intensity within each (annular) ellipse was found and calibrated with the determined photometric zeropoint.

Surface brightness profiles were then plotted against the major axis (in arcsec). A best fit line was found, typically using the exponential profile:

$$\Sigma(\mathrm{r}) = \Sigma_0 \, \mathrm{e}^{-\frac{\mathrm{r}}{\alpha}} \tag{1}$$

where Σ_0 is the central surface brightness of the disk in linear units ($M_\odot$ /pc^2), and α is the exponential scale length in arcsec. This can also be written

$$\mu(\mathrm{r}) = \mu(0) + (\frac{1.086}{\alpha})\mathrm{r} \tag{2}$$

where $\mu(0)$ is the central surface brightness in (mag arcsec^{-2}).

In some cases, the exponential fit was clearly a bogus representation of the light profile. In these cases, we found that the surface brightness profiles were much better fit (in the reduced χ^2 sense) with King's (1965) model of star clusters, approximated by:

$$\mu(\mathrm{r}) = \mu(0) + 2.5\log(1 + (\frac{\mathrm{r}}{\mathrm{R_E}})^{\mathrm{n}}) \tag{3}$$

where $\mu(0)$ again is the central surface brightness in (mag arcsec^{-2}), $\mathrm{R_E}$ is the core radius, and n is a free parameter. The inner 2" of each profile was ignored (due to seeing effects) for the fit, as were the outer radii with errors greater than 0.25 mag arcsec^{-2} .

To verify our method, it was applied to various known galaxies in our fields, and the final colors and surface brightness distributions were checked against other published values (Bothun, et al 1985, Caldwell & Bothun 1987, Sandage & Visvanathan 1978, Longo & de Vaucouleurs 1983) All values were found to be within the other papers' error, giving an accuracy on the total magnitudes and central surface brightness of 0.1 mag.

For these data, average sky brightness through the blue filter was 21.8 $\pm$ 0.3 μ_B , brighter than expected due to a persistent layer of cirrus clouds in the sky. (On clear nights the sky brightness fell to 22.5 μ_B .) Galaxies with a central surface brightness as faint as 26.0 μ_B (3% of the sky background) were detected, and an accurate (error $\leq$0.25 mag arcsec^{-2}) radial surface brightness distribution was typically found to 27.0 μ_B (1% of the sky background), or fainter on the darker nights.

Galaxy inclination was found by using the GASP software to determine the major and minor axis at each isophote. The inclination angle is then:

$$i \ = \ \cos^{-1}\frac{\mathrm{r_{minor}}}{\mathrm{r_{major}}} \tag{4}$$

but we estimate that i is accurate only to within 5.0 °due to the non-elliptical nature of the LSB galaxies and their varying axis ratio for each annulus.

Finally, precisely because they are LSB galaxies, the galaxy size was determined using the 27 μ_B isophote as the reference level, and not to the 25 μ_B isophote as is commonly done in

HSB galaxy surveys. For a typical LSB galaxy, 25 μ_B encloses less than 2 scale lengths of disk light.

5. The Data

The surface brightness profiles for all of the galaxies are shown in figure 13, along with their best-fit curve (when applicable). The profiles are for the images through the blue filter when possible (runs 1,2,3 & 5), and otherwise through the visual filter (run 4). When more than one best-fit curve is shown, the data listed in the corner of the graph is for the outer disk of the galaxy and is the information used in tables 2-5. If the galaxy equation type is 's', an exponential was fit to the data, in accordance with equation 2. When the galaxy equation type is given as 'k', a king profile was used (equation 3).

Table 2 lists all the galaxies with surface brightness $\geq$22.0 $\mu_B(0)$ for all fields but those taken 10/26/95-10/30/95. Galaxies with central surface brightness $\geq$21.5 $\mu_V(0)$ from those days are listed in table 3. Table 2 is organized as follows:

Column 1: Galaxy names as used in this paper. These correspond to our internal field sequencing convention.

Column 2: Other names for the galaxy, where a prefix of UGC is from Nilson (1973), KUG from Takase & Miyauchi-Isobe (1993), and [KK] is from Karachentsev & Kopylov (1990). If this column is blank the galaxy is previously unidentified.

Columns 3-4: Right ascension and declination of the galaxies, accurate to within 10". To find the galaxies' position, known objects within the field were identified, and their location within the field was used to determine the coordinates of the field center (using our measured scale of 1.32"/pixel). The pixel coordinates for the center of each LSB galaxy in the field was then found (using IRAF's IMCENTER procedure) and converted to equatorial (1950) coordinates.

Columns 5-6: Blue magnitude of the galaxy both at 5" and the total magnitude. Magnitudes are corrected for Galactic extinction but not for either inclination or redshift. Magnitudes are quoted to within 0.05 mag.

Column 7: The total integrated blue magnitude for the galaxy is calculated using

$$\mathrm{mag}(\alpha) \;=\; \mu(0) \;-\; 2.5\log\left(2\pi\alpha^2\right) \tag{5}$$

where α is the exponential scale length in arcsec. No correction was made for internal reddening due to the (presumed) low dust content of most LSB galaxies. If an exponential could not be fit to a particular galaxy's surface brightness profile, this column is left blank.

Column 8: The central surface brightness in mag arcsec^{-2} , as defined in section 4, with error of 0.05 μ_B .

Column 9: The inclination-corrected central surface brightness in mag arcsec^{-2} . $\mu_B(0)\ _c$=$\mu_B(0)$ -2.5log(cos(i)), where the inclination used is listed in column 10. Note this is a geometric path length correction which assumes no dust (see also section 8).

Column 10: The inclination angle (in degrees) as found by the GASP software. The angle is correct within $\pm$ 5. $^\circ$. (The error is due primarily to the LSB galaxies' clumpy shapes.)

Columns 11-12: The exponential scale length in both arcsec and kpc. Since redshifts are not currently known, the conversion from arcsec to kpc was based on an average distance either to the cluster (Pegasus or Cancer) or to the primary galaxy in the image (i.e. NGC 3344). The angular exponential scale length has a small error

(0.05 "); α and m(α) are not given either for galaxies with a King profile of for galaxies whose surface brightness profile is too irregular for a linear fit.

Columns 13-14: The major axis radius in arcsec, measured at the 27.0 μ_B and 25.0 μ_B isophotes. If the surface brightness profile errors exceeded 0.25 mag arcsec^{-2} before $\mu_B = 27$ mag arcsec^{-2} , then the largest accurate radius is given in place of r_{27}.

Table 3 gives the surface brightness information and structural characteristics for the data taken 10/26/95-10/30/95. As no information was available for these galaxies in the blue, all structural information was found through analyzing the galaxies in the V filter. The data in table 3 was obtained through the same methods as that in table 2, and table 3's layout is also the same.

6. Central Surface Brightness

The majority of the LSB galaxies found (102 galaxies - 80%) had surface brightness profiles well fit by an exponential disk (shown in logarithmic units in equation 2). The rest of the galaxies were either fit by a king profile (21 galaxies - 17%) or were too clumpy to be fit by any curve (4 galaxies - 3%).

The galaxies best fit by a king profile typically have $2.0 \leq$n ≤ 5.0 ($\langle$ n $\rangle = 3.98 \pm .27$), and have core radii between 5.0" and 10.0" ($\langle$rcore$\rangle = 7.35 \pm .38$). No relationship is evident between n, the core radius, or the central surface brightness. (See figure 2 (a) and (b).) LSB galaxies with these kinds of structural parameters have never been detected before outside of the Local Group. The observed angular core radii are similar to those observed for many Galactic Globular Clusters whose profiles are well fit by a King model. This raises the possibility that these objects are, in fact, LSB globular clusters. The distribution of their ellipticities shows two distinct classes - those with an inclination around 40° and those with an inclination around 66° (figure 3). The average values of the two groups are $\langle\ i\ \rangle = 38.2 \pm\ 2.5°$ and $\langle\ i\ \rangle = 67.6 \pm\ 3.3°$. It is possible that the more elliptical objects have been tidally flattened. Alternatively, these objects could be a new kind of highly inclined LSB galaxies (which means if they were observed face-on $\mu_B(0)$ would likely be below our detection threshold) which happen to have a light profile better defined by a King model than an exponential one. Clearly the nature of these objects will remain ambiguous until redshifts are acquired. For now we do note that some LSB globular clusters have been previously found (i.e. see Djorgovski & Meylan 1994, Racine 1975), and perhaps our survey has added a significant quantity to the total number of LSB globular clusters.

One circumstantial way to determine if the LSB objects in the Pegasus and Cancer fields are cluster members is to plot total magnitude (B) versus central surface brightness. As shown in Bothun et al (1989), a tight relation will result if the sample has similar intrinsic scale length. The data are shown in figure 4 for the Pegasus (squares) and Cancer (crosses) fields. A linear relation between $\mu_B(0)$ and $\mathrm{B_T}(0)$ is evident which shows that the galaxies are at (roughly) the same distance and therefore that true LSB cluster members have not been selected against by our diameter criterion.

The distribution of central surface brightness for all galaxies found with surface brightness $\geq$22.0 $\mu_B(0)$ is shown in figure 5. $\mu_B(0)$ for galaxies for which no blue data is available (those galaxies detected in the 10/26/95-10/30/95 data) was determined using

$$\mu_{\mathrm{B}}(0) = \mu_{\mathrm{V}}(0) + 0.50\ \mathrm{mag/arcsec^{-2}} \tag{6}$$

The observed surface brightness distribution is reasonably flat until 24.0 $\mu_B(0)$ (25.0 $\mu_B(0)$ for the inclination corrected sample - see figure 7), where a sharp drop-off is observed. This drop-off occurs well before the detection threshold of $\mu_B(0)$ $\sim$26.5 mag arcsec^{-2} .

Overlayed atop the surface brightness distribution are the probability curves for this sample, based on distance (volume) based selection effects, which are proportional to

$$\mathrm{N}(\mu_{\mathrm{B}}(0) \propto (\mu_{\mathrm{L}} - \mu_0)^3$$

(See OBCI for more details on the probability distribution.) The curves are normalized to the average of $\mathrm{N}(\mu(0)$) over the range 22.0 mag arcsec^{-2} $\leq\mu_B(0)$ lta 23.5 mag arcsec^{-2} . The solid curve is for $\mu_{\mathrm{L}} = 26.0$ mag arcsec^{-2} , while the dashed and dashed-dotted lines are for $\mu_{\mathrm{L}} = 26.5$ mag arcsec^{-2} and $\mu_{\mathrm{L}} = 27.0$ mag arcsec^{-2} , respectively. Even in the most extreme case, with $\mu_{\mathrm{L}} = 26.0$ mag arcsec^{-2} , a deficiency in galaxy counts for 23.5 mag arcsec^{-2} $\leq\mu_B(0)$ $\leq$24.5 mag arcsec^{-2} is obvious. In the more realistic case of $\mu_{\mathrm{L}} =$ 26.5 mag arcsec^{-2} – the $\mu_{\mathrm{L}} = 26.0$ mag arcsec^{-2} case does not allow for the existence of the $\mu_B(0)$ $\geq$25.5 mag arcsec^{-2} – the deficiency becomes even more pronounced. The observed drop-off, then could not be the result of surface brightness selection effects. These objects are simply rarer in our survey compared to those observed with 22.0 $\leq\mu_B(0)$ $\leq$24.0. Similarly, our observations show no apparent difference between the surface brightness distribution for the galaxies found in the Pegasus and Cancer fields from those found in the other, occasionally more distant, clusters (figure 6), nor is there any difference between the $\mu_B(0)$ versus α distribution for the various survey ares (figure 8). This indicates that distance effects are not limiting our survey sample and thus are not the cause of the drop in the surface brightness distribution.

One possibility for the observed distribution of $\mu_B(0)$ is the inability for extremely LSB galaxies to form in a cluster environment. Some evidence for this is shown in figure 9 which is a physical expression of the morphology-density relation of Dressler (1980). Here we plot the total (2-dimensional) galaxy density for each field against the average $\mu_B(0)$ for that field. The data suggest that the lowest central surface brightness attainable within an environment is limited by total galaxy density. The only exception is at a galaxy density of approximately 0.2, the field surrounding NGC 4526. Most likely this is due to our lack of redshifts for the galaxies giving us an incorrect field density and is not an exception to the trend. A similar result can be seen in figure 10, which shows the average galaxy size (in kpc) per field versus the total galaxy density for each field. Again a trend toward smaller galaxies with higher densities is evident. Thus the conclusion that the observed distribution fall-off at 24.0 $\mu_B(0)$ results from LSB galaxies not being able to survive in the density of cluster environments is supported by the data. When the Arecibo telescope is fully re-furbished we plan to acquire redshifts of all the sample galaxies to confirm these results.

These environmental dependencies are consistent with those found in an earlier study by Bothun et al (1993) who claimed a deficit of nearby galaxies within a 0.50 Mpc/500 km sec^{-1} radius around LSB disk galaxies when compared to HSB disk galaxies, and an average nearest-neighbor distance 1.7 times farther than for HSB galaxies. Their findings are consistent with the interpretation that the low surface mass density of LSB galaxies (de Blok et al 1996) results in LSB galaxies being strongly influenced by the gravitational pull of nearby galaxies. Thus, whether it is due to tidal interactions ripping the very low surface density galaxies apart or to the same interactions triggering star formation and thus the collapse of the galaxies into denser, brighter objects, thereby raising the surface brightness, the fall-off in this survey at 24.0 $\mu_B(0)$ is the result of the LSB galaxy's difficulty in surviving a cluster's dense environment. This statement, however, is somewhat difficult to reconcile with the recent claim by Ulmer et al (1996) for the existence of very LSB galaxies in the core of the Coma cluster.

7. The Surface Brightness Profiles

In general, surface photometry of LSB galaxies is rather difficult. Although many of the galaxies in our sample are well fit by either an exponential surface brightness profile (eq. 2) or a king profile (eq. 3) there are some notable exceptions. In many cases, there is a lot of "noise" superimposed on the basic underlying structure. This noise is a manifestation of the very clumpy structure of some LSB galaxies. In these cases, the galaxy morphology is defined by small bright clumps surrounded by much fainter regions. This can result in a light distribution which is somewhat non-continuous. The low signal-to-noise ratio of the fainter regions, combined with this lack of any well-defined central galactic core results in the surface brightness profiles that are "bumpy" and irregular. Of the ten galaxies in this survey which fall into this category, two (P5-5 & N1-3) show the effects of this clumpiness only in the inner part of the galaxy (the inner 8" and 5", respectively). A reasonably good surface brightness profile could then be fit to the outer regions of the two galaxies. Five (C4-8, C5-3, C11-3, N3-2, and N10-5) retain enough of a linear profile for a best-fit line to be found, although in all five cases the error for both $\mu_B(0)$ and α is fairly high. Three more (P9-4, C4-7, & C10-1) simply cannot be fit by either a linear profile or a king profile.

In some other cases either scattered light from a nearby bright star or a low signal-to-noise ratio detection of the LSB itself precludes accurate surface photometry. Although we attempted to mask all the stars and other flaws in each galaxy's foreground, we were not always completely successful, either because of the flaw's large size relative to the galaxy or because the star is not distinguishable from a faint clump of light that could be part of the galaxy. Both N6-4 and N5-2 have large bumps in their surface brightness profiles (at 20" and 5", respectively) that reflect this ambiguity. C4-6 has a foreground star which, because of C4-6's large inclination ($i \approx$ 60-65°), effectively prohibits us from obtaining any information about its photometry. P4-4 has a large bump in its surface brightness profile (before 5") due to contamination from a foreground star.

For a few galaxies, there is a clear ambiguity about what should be defined as the center. In these cases, the peak pixel intensity is rather far offset from the centroid of the light distribution as defined by the fainter, outer isophotes. Such a case could arise from a single H II region in a small LSB galaxy. The cases of P3-4, U1-3 and N6-3 reflect this situation and there is a discontinuity in their light profiles at r $\sim$5 ". In other cases, the discontinuity manifests itself in the appearance of two exponential profiles for the galaxy - an inner and outer profile. Although it is common for HSB galaxies to have two separate profiles, a de Vaucouleurs ($r^{1/4}$) type of bulge profile and a exponential disk profile (de Vaucouleurs 1959), most of the LSB galaxies in this survey lack a bright central bulge and none have an inner ($r^{1/4}$ profile type) bulge. In the case of both P2-3 and C1-1, the inner and outer components of the galaxy are both accurately fit by separate exponential profiles. P1-1 is fit by an inner exponential profile and an outer king profile. These inner 'bulges' may represent the kind of secular disk evolution resulting in inner 'starpiles' of material that has been described by Kormendy (1996).

8. Other Structural Properties

Although the average inclination for the galaxies in this survey is i=50° , their actual values cover a wide range - from i= 19° through i=85° . The face-on galaxies are of note because they both provide the best opportunity for observing structure in these LSB galaxies and they give us an unobscured surface brightness profile. The discovery of edge-on LSB galaxies in this sample provides an important constraint for models of faint galaxy counts (see Ferguson & McGaugh 1995). Very little is known about the dust content of LSB systems other than H II region spectroscopy which does show some Balmer Decrement (see McGaugh 1992). The generally blue colors of LSB disks (*e. g.* McGaugh & Bothun 1994), coupled with their low metallicity provides circumstantial evidence for low dust content.

However, the large range in inclination of this sample allows for a simple test to be made.

In figure 11 we perform this simple test. If dust opacity in optically thin LSBs disks is important, we might see a correlation between galaxy inclination and central surface brightness. In the no dust case, the correction is the geometrical path length correction that produces a difference of 2.5 mags between edge-on and face-on disks. While Figure 10 is not a rigorous test, given the intrinsic range of $\mu_B(0)$, the non-correlation is remarkably similar to the non-correlation between inclination and $\mu_B(0)$ that is observed for samples of HSB. In the past this non-correlation has been used as an argument that HSB disks are optically thick (*e. g.* Valentijn 1991; Simien et al 1993). The same situation is clearly seen here, but it would be rather absurd to conclude from Figure 10 that these extremely low density systems, which are devoid of molecular gas (see Schombert et al 1990) are optically thick!

A recent paper (Cowie et al 1995) claims to have found a new class of galaxies - 'chain galaxies' which are high redshift galaxies that appear to be very thin. Cowie et al argue that 'these very large ellipticities argue strongly against these being any class of edge-on object' and that the lack of low redshift counterparts to their chain galaxies warrant placing these galaxies in a new morphological class. The axial ratios (a/b) given by Cowie et al , though, lie between 2.0 and and 9.5, which correspond only to inclinations between 60° and 84° . Numerous galaxies in our survey have $i > 60°$ and a few with inclinations greater than 80° . Dalcanton & Schectman (1996) similarly have found a large number of extremely thin, LSB galaxies at redshift z $\approx$ 0.30. (Both the galaxies in our survey and in the survey of Dalcanton & Schectman also show hints of the 'knots' evident in Cowie et al 's sample.) The existence of numerous galaxies with $i \geq 60$ ° and the continuous distribution of LSB galaxy inclinations in our survey through $i \geq 80°$ argue strongly that Cowie et al have not found a new galaxy morphology but instead examined a group of edge-on LSB galaxies which happen to be at high redshift.

The size of the galaxies in this survey are smaller on average than those of other LSB and HSB surveys. The average scale length for the galaxies in this survey is 7" or 1.5 kpc, and the average r_{27} is 19.6 $\pm$ .8" (see figure 1). The range is 0.078 kpc$\leq$h $\leq$4.3 kpc. Previous LSB surveys have had $\langle$h$\rangle$=3.2 kpc with a typical range of 0.3 kpc $\leq$h $\leq$10 kpc, (de Blok, et al 1995, McGaugh & Bothun 1994). HSB galaxy surveys typically have 0.5 kpc $\leq$h $\leq$7kpc (van der Kruit 1987, de Jong 1995). That the LSB galaxies in this survey lie only in the (h $\leq$4.5 kpc) end of the galaxy sizes agrees well with the argument that in a cluster environment tidal interactions limit the size LSB galaxies can attain.

Finally, four of the galaxies with $i < 35°$ clearly show the various extremes in galaxy shape for LSB disk galaxies (figure 11 but these galaxies are best reproduced in the on-line LSB gallery located at http://zebu.uoregon.edu/sb.html). The most structurally distinct galaxy in our survey is P1-7. Like most LSB disk galaxies P1-7 is a late-type spiral galaxy (Hubble type Sm), but unlike most of the galaxies in this catalog, P1-7 clearly shows its spiral structure. Having $\mu_B(0)$ = 23.08 mag arcsec^{-2} , combined with its bright bulge, P1-7 was easily identified during our galaxy search. The other three galaxies range from slightly less distinct than P1-7 to complete amorphous blobs. Barely showing its spiral arms, C9-1 bridges the gap between P1-7 and the more amorphous LSB galaxies. Along with the fading of its distinct spiral structure, C9-1 also lacks P1-7's distinct central bulge. N10-4 still has an obvious central region, but beyond that no distinctive structure can be seen in it. N10-4 has a central surface brightness of 24.05 $\mu_B(0)$, and a size of only r_{27} = 10.76 ". Finally, N10-5 is an example of a very low signal-to-noise LSB galaxy. With a central surface brightness of 23.85 $\mu_B(0)$ and its lack of any central light concentration it was one of the more difficult galaxies to properly identify.

9. Summary

During this survey we found 129 LSB galaxies, 119 of which were previously uncatalogued. Of these only six (P2-4, P9-3, C11-3, N1-3,N10-5 & N3-2) have $\mu_B(0) > 24.5$ mag arcsec^{-2} and fall into the category of very LSB galaxies. Nonetheless, the average central surface brightness for our total sample is 23.06$\pm$ 0.20 $\mu_B(0)$, more than 4 standard deviations from Freeman's (1970) value of 21.65 $\pm$ 0.3 $\mu_B(0)$. More significant is the flat distribution through 24.0 $\mu_B(0)$, 7 deviations and more than 2 magnitudes fainter than Freeman's value. In agreement with past findings (i.e. Romanishin, et al 1983, Impey et al 1988, Schwartzenberg, et al 1996), it is evident Freeman's value is not representative of the overall galaxy population but most likely is the result of serious selection effects (see Disney 1976, Disney & Phillips 1983, McGaugh, et al 1995b).

Though we lack redshifts, the structural components of the galaxies are consistent with them having redshifts between 3000 and 8000 km sec^{-1} ; that is, it is unlikely that many of these LSB objects are nearby, low mass dwarf galaxies. One surprising find in this paper is the number of LSB galaxies with a profile fitting King's (1965) model for globular clusters. The possibility that we have found a class of LSB globular clusters is good. In addition, as we more fully discuss in OBCI, this new CCD survey has resulted in the discovery of LSB galaxies that are significantly redder than those detected in previous surveys. This is most reassuring as the simplest of all arguments suggests that disk galaxies must fade and redden as the Universe ages. Surely, after t ~15 billion years, some of this fading must have occurred by z =0.

For this sample no relation exists between the LSB galaxies' inclination and central surface brightness. If we apply a geometrical path length correction to convert the observed $\mu_B(0)$ to its face-on value (see Figure 6), galaxies as faint as $\mu_B(0) = 27.1$ mag arcsec^{-2} were detected. At the same time a significant number of LSB galaxies with $i > 60°$ (and even $i > 80°$) was found, galaxies which fall into Cowie et al 's (1995) classification of 'chain galaxies'. As a smooth distribution of inclinations from $30° \leq i \leq 85°$ is evident it is doubtful that the $i > 60°$ galaxies are a new morphological class of galaxies - instead they are just highly inclined, yet otherwise typical, LSB galaxies.

Finally, it was shown that within the cluster environment of our survey, a sharp drop-off in the number of galaxies with $\mu(0) \geq 24.0\ \mu_B(0)$ is evident. Although many possibilities exist to explain this drop-off, the most compelling argument is that extremely LSB galaxies have difficulty existing in dense environments. The tidal forces within galaxy clusters that aid the development of reasonably compact galaxies rip apart those galaxies more lacking in density - the very LSB galaxies. This idea is supported by the trend towards fainter surface brightnesses appearing in the less dense regions of space. More evidence towards this conclusion will be presented in OBCI.

This research has made use of the NASA/IPAC extragalactic database (NED) which is operated by the Jet Propulsion Laboratory, California Institute of Technology, under contract with the National Aeronautics and Space Administration. The authors would like to thank David Chappell and Niall Gaffney for their help in acquiring the observations described here.

References

Bothun, G., et al . 1993, AJ, 106, 530

Bothun, G., et al . 1991, ApJ 376, 404

Bothun, G., Shombert, J., & Caldwell, N. 1989, AJ, 98, 1542

Bothun, G., et al . 1987, AJ, 94, 23

Bothun, G, et al . 1985, ApJS, 57, 423

Bothun, G, et al . 1982, AJ, 87, 725

Caldwell, N. & Bothun, G. 1987, AJ, 94, 1126

Cawson, M. 1983, Ph.D. thesis, University of Cambridge.

Claver, C. 1995, Ph.D. thesis, University of Texas at Austin.

Cowie, L, Hu, E., & Songalia, A. 1995, AJ, 110, 1576

Dalcanton, J. & Schectman, S. 1996, ApJ, 465, 9

De Blok, W., McGaugh, S. & van der Hulst, J. 1996 MNRAS, preprint

De Blok, W., Bothun, G, & van der Hulst, J. 1995, MNRAS, 274, 235

De Jong, R. 1995, PhD thesis, Rijksuniversiteit, Groningen

Dell'Antonio, I, Geller, M., & Bothun, G. 1996, AJ, in press

De Vaucouleurs, G. 1959, in *Handbuch der Physik, v. 53, Astrophysics and Stellar Systems*, (ed. S. Flügge. Berlin: Springer-Verlag)

Disney, M. 1976, Nature, 263, 573

Disney, M. & Phillipps, S. 1983, MNRAS, 205, 1253

Djorgovski, S. & Meylan, G. 1994, AJ, 108, 1292

Dressler, A. 1980, ApJ, 236, 351

Ferguson, H. & McGaugh, S. 1995, ApJ, 440, 470

Freeman, K. 1970, AJ, 160, 811

Geller, M., & Huchra, J. 1989, Sci, 246, 897

Impey, C., & Bothun, G. 1997, ARAA, in preparation

Impey, C., et al . 1996, ApJS, 105, 209

Impey, C., Bothun, G., Malin, D. 1988, ApJ, 330, 634

Karachentsev, I., & Kopylov, A. 1990, MNRAS, 243, 390

King, I. 1965, AJ, 71, 64

Kormendy, J. 1996, *IAU Symposium 153, Galactic Bulges*, preprint

Landolt, A. 1983, AJ, 88, 439

Landolt, A. 1973, AJ, 78, 959

Longo, G. & de Vaucouleurs, A. 1983, *A General Catalogue of Photometric Magnitudes and Colors in the U,B,V System of 3,578 Galaxies Brighter than 16-th V-magnitude,* (University of Texas Astronomy Monographs, No.3)

Malin, D. 1978, Nature, 276, 591

McGaugh, S. 1996, MNRAS, 280, 337

McGaugh, S. 1992, Ph.D. thesis, Michigan University, Ann Arbor

McGaugh, S., Schombert, J. & Bothun, G. 1995a, AJ, 109, 2019

McGaugh, S., Bothun, G.,& Schombert, J. 1995b, AJ, 110, 573

McGaugh, S., & Bothun, G. 1994, AJ, 107, 530

Nilson, P. 1973, *Uppsala General Catalog of Galaxies*, (Stockholm: Almquist & Wiksell)

O'Neil, K., Bothun, G., Cornell, M. , and Impey, C. 1996, in preparation

Racine, R. 1975, AJ, 80, 1031

Romanishin, K., Strom, K., & Strom, S. 1983, ApJS, 53, 105

Sandage, A., Visvanathan, N. 1978, ApJ, 223, 707

Schwartzenberg, J. et al 1996, A&AS, 117, 179

Schombert, et al 1992, AJ, 103, 1107

Schombert, et al 1990,AJ, 100, 1523

Simien, F., Morenas, V., & Valentijn, E. 1993, A&A, 269, 111

Sprayberry, D., et al 1996, ApJ, 463, 535

Takase, B. & Miyauchi-Isobe, N. 1993, Publ. Nat. Astron. Obs. Japan, 3, 169

Ulmer, M., et al 1996, AJ, in press

Van der Hulst, J. M., et al 1993, AJ, 106, 538

Van der Kruit, P. 1987, A&A, 173, 59

Zwicky, F. 1961, *Catalogue of Galaxies and Clusters of Galaxies.* (Pasadena: California Institute of Technology)

Figure 1. Histogram of r_{27} (in arcsec) for all of the galaxies in our survey. The galaxies were selected (by eye) to have a minimum radius of 10 pixels (13.2")

Figure 2. Plots of (a) the core radius (in ") versus n and (b) the central surface brightness (in mag arcsec^{-2}) vs. the core radius for all of the galaxies in the survey with a surface brightness profile matching the king curves (equation 5).

Figure 3. Histogram showing the distribution of inclination angles for both the galaxies fitting a king-type surface brightness profile (dotted line) and a linear surface brightness profile (solid line).

Figure 4. Total blue magnitude versus central surface brightness (in mag arcsec^{-2}) for the galaxies found in the Pegasus (squares) and Cancer (crosses) fields in our survey.

Figure 5. The central surface brightness distribution for all galaxies in this survey. $\mu_B(0)$ for those galaxies without an image in the blue were found using equation 5. Overlayed on the histogram are is the probaility distribution for finding galaxies at the various surface brightnesses, normalized to N($\mu(0)$) $\approx$ 13.6, the avarage of N($\mu(0)$) over 22.0 mag arcsec^{-2} $\leq\mu_B(0)$ lta 23.5 mag arcsec^{-2} . The solid line is for $\mu_{\rm L}(0) = 26.0$ mag arcsec^{-2} , while the dotted and dashed dotted lines are for $\mu_{\rm L}(0) = 26.5$ mag arcsec^{-2} and $\mu_{\rm L}(0) = 27.0$ mag arcsec^{-2} , respectively.

Figure 6. Normalized histogram comparing the central surface brightness distribution of galaxies found in the Pegasus cluster (solid line), Cancer cluster (dashed line), and near various single galaxies (all other data) (dash-dotted line). If no blue surface brightness data was available for the galaxies, $\mu_B(0) = \mu_V(0) + 0.5$mag arcsec^{-2} was used.

Figure 7. Normalized histogram comparing the inclination corrected central surface brightness distribution of galaxies found in the Pegasus cluster (solid line), Cancer cluster

(dashed line), and near various single galaxies (all other data) (dash-dotted line). Inclination correction was done using $\mu_B(0)$ (corrected)=$\mu_B(0)$ - 2.5log(cos$i$). If no blue surface brightness data was available for the galaxies, $\mu_B(0) = \mu_V(0) + 0.5$mag arcsec^{-2} was used.

Figure 8. $\mu_B(0)$ versus scale length (in arcsecs) for all the galaxies in our survey. Galaxies found in the Pegasus cluster are represented by squares, galaxies found in the Cancer cluster are represented by xs, and all other galaxies by triangles. No difference is apparent in this distribution for the various survey areas.

Figure 9. Total galaxy density in each field (in number/kpc^2) versus the average central surface brightness of each galaxy field is shown. The exception to the downward trend in central surface brightness is the field surrounding NGC 4526, at a density of ~ 0.2.

Figure 10. Total galaxy density in each field (in number/kpc^2) versus the average exponential scale length (in kpc) for each field is shown. (See equation 1.) A trend toward smaller galaxy size with increasing field galaxy density can be seen.

Figure 11. Galaxy inclination (in degrees) versus central surface brightness for the galaxies in our survey. The solid lines are the average values for both variables. Note that no correlation is apparent between the two variables.

Figure 11. Inverted images of select galaxies in our survey. The images are shown to display the varying structure in LSB galaxies. Left to Right, starting at the top, the images are: P1-7, a LSB galaxy with distinct spiral structure; C9-1, which still shows some structure but lacks P1-7's central bulge; N10-4, typical LSB galaxies for this survey; and N10-5, a galaxy whose low central surface brightness and lack of any central concentration, made it one of the more difficult galaxies to identify.

Figure 12. The surface brightness profiles for all the galaxies included in our survey. The surface brightness profiles shown are in B for all galaxies except those galaxies listed in table 3, when no blue information was available. In these cases, the V data was used instead. (Filter used for the surface brightness profiles are given in parenthesis after the galaxy name.) Unusual surface brightness profiles are discussed in section 6 of the paper.

Table 1: Central field object(s) and coordinates, field areas, and dates for all of the observations in this paper.

Table 2: Derived information on all galaxies with central surface brightness $\geq$22.0 $\mu_B(0)$ except for the fields taken 10/26/95-10/30/95. See section 5.

Table 3: Derived information on all galaxies with central surface brightness $\geq$21.0 $\mu_V(0)$ or the fields taken 10/26/95-10/30/95. See section 5.

Table 1: Central field objects and coordinates, field areas, and dates for all of the observations in this paper.

Sky Area	**Central Coords (1950)**	**Field Area**	**Dates taken**
Pegasus Cluster	23:16:30, 7:55:0	180'x180'	1,3
Cancer Cluster	8:12:54, 21:14:30	180'x150'	1,2,3
AWM3	14:24:02, 26:12:49	45'x45'	2
IC 2574	10:25:00, 68:46:42	80'x60'	4
IC 4574	15:39:45, 28:21:56	45'x45'	5
NGC 205	00:38:06, 4:29:42	60'x60'	4
NGC 925	02:23:42, 33:21:48	50'x60'	4
NGC 2146	06:10:37, 78:21:03	45'x45'	1
NGC 3204	10:17:24, 28:01:52	45'x45'	5
NGC 3344	10:41:04, 25:10:54	45'x45'	2
NGC 3493	10:58:49, 27:59:05	45'x45'	5
NGC 4526	12:31:35, 07:58:39	45'x45'	2
NGC 4585	12:34:50, 29:14:20	45'x45'	5
NGC 5081	13:16:47, 28:46:09	45'x45'	5
NGC 5711	14:37:06, 20:14:22	45'x45'	5
NGC 6946	20:33:12, 59:53:18	80'x45'	4
TDSS 0432-0110	4:33:59, -01:15:261	45'x45'	1
UGC 6614	11:36:39, 17:24:47	45'x45'	2

Dates: (1) 10/14-18/93, (2) 3/7-12/94, (3) 10/29/94-11/3/94, (4) 10/26/95-10/30/95 (5) 4/12/96-4/17/96

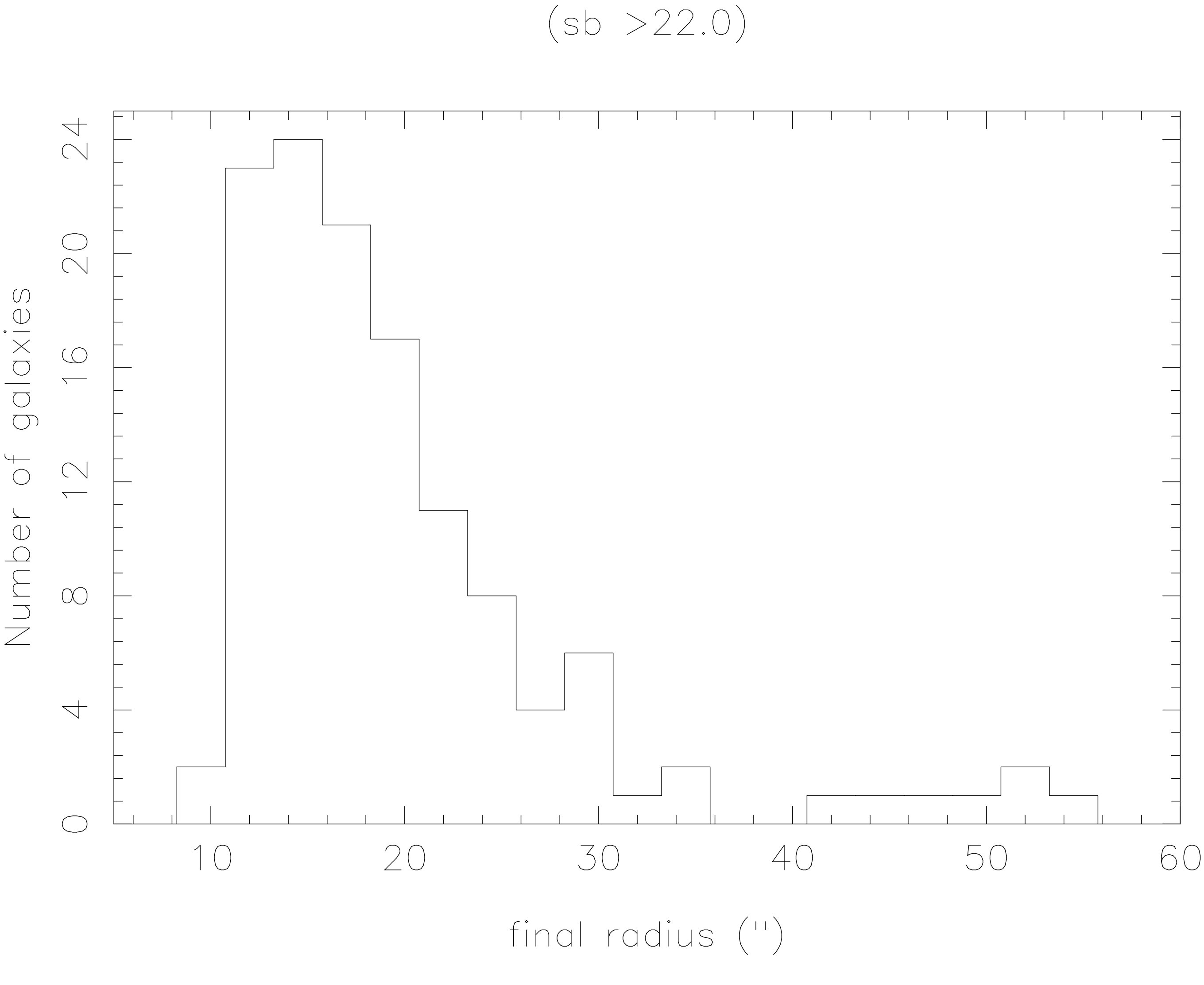
(sb >22.0)
Number of galaxies
0
4
8
12
16
20
24
10
20
30
40
50
60
final radius ('')

Fig. 1.—

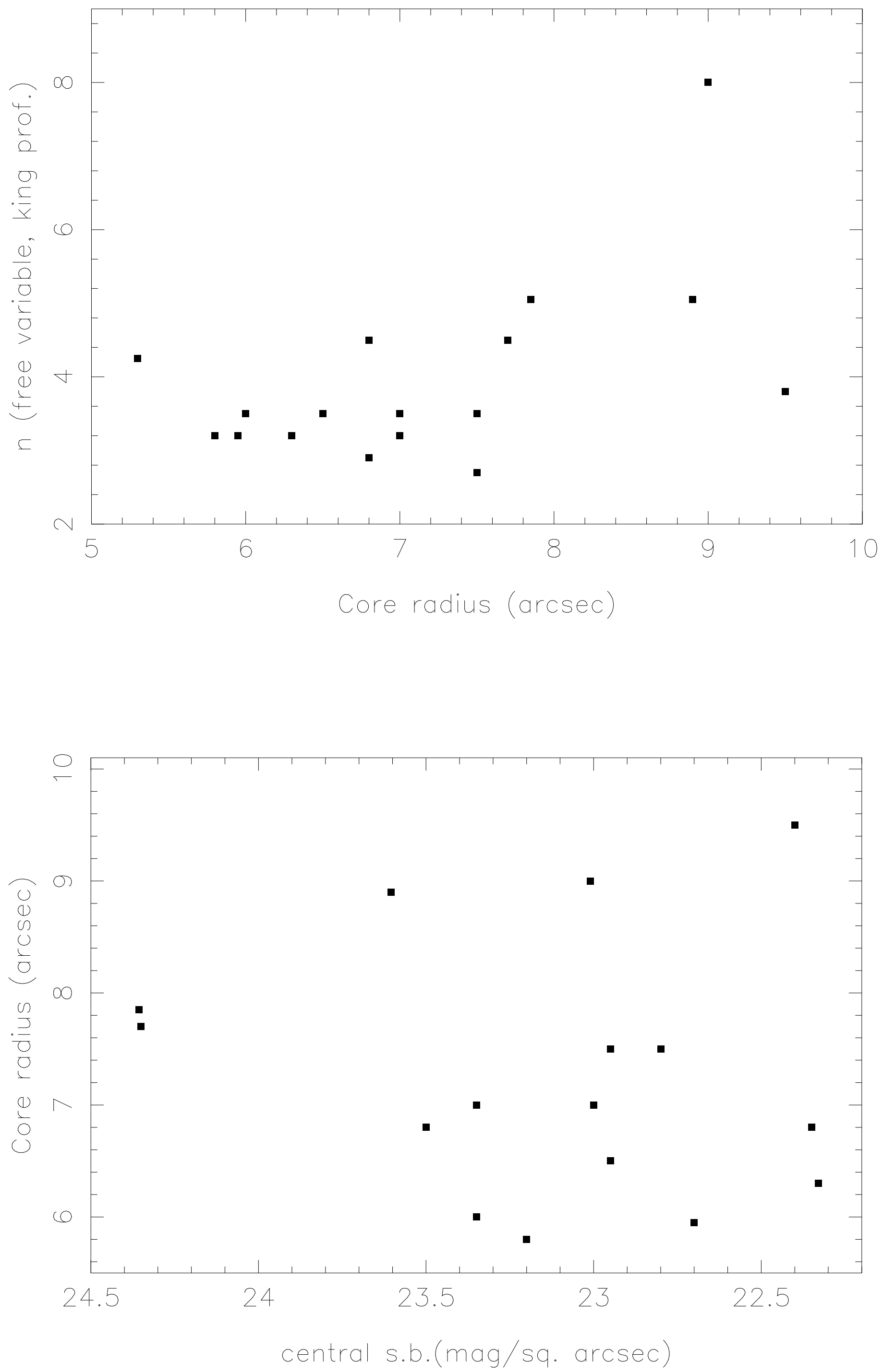
n (free variable, king prof.)
Core radius (arcsec)
Core radius (arcsec)
central s.b.(mag/sq. arcsec)

Fig. 2.—

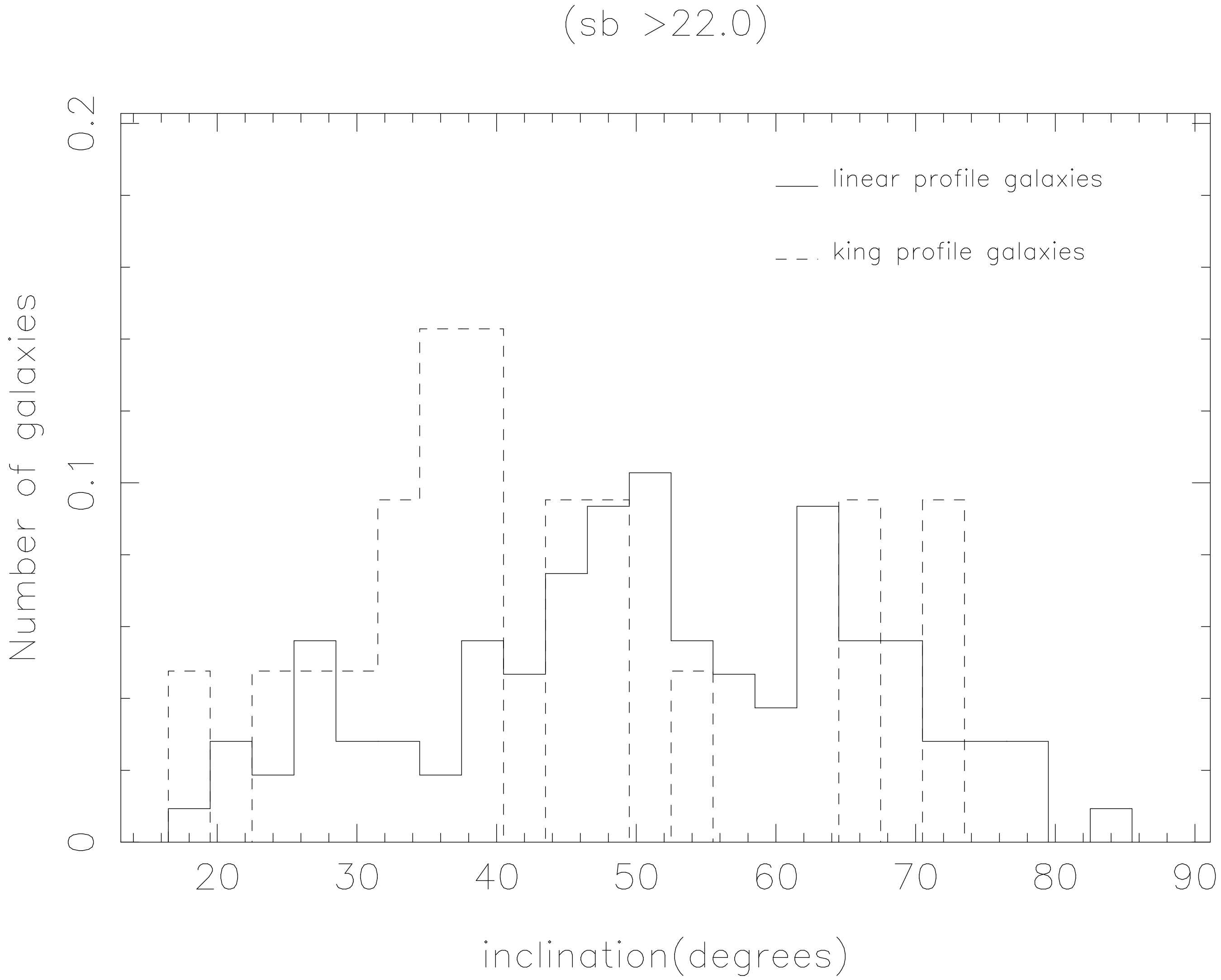

(sb >22.0)
linear profile galaxies
king profile galaxies
Number of galaxies
0
0.1
0.2
20
30
40
50
60
70
80
90
inclination(degrees)

Fig. 3.—

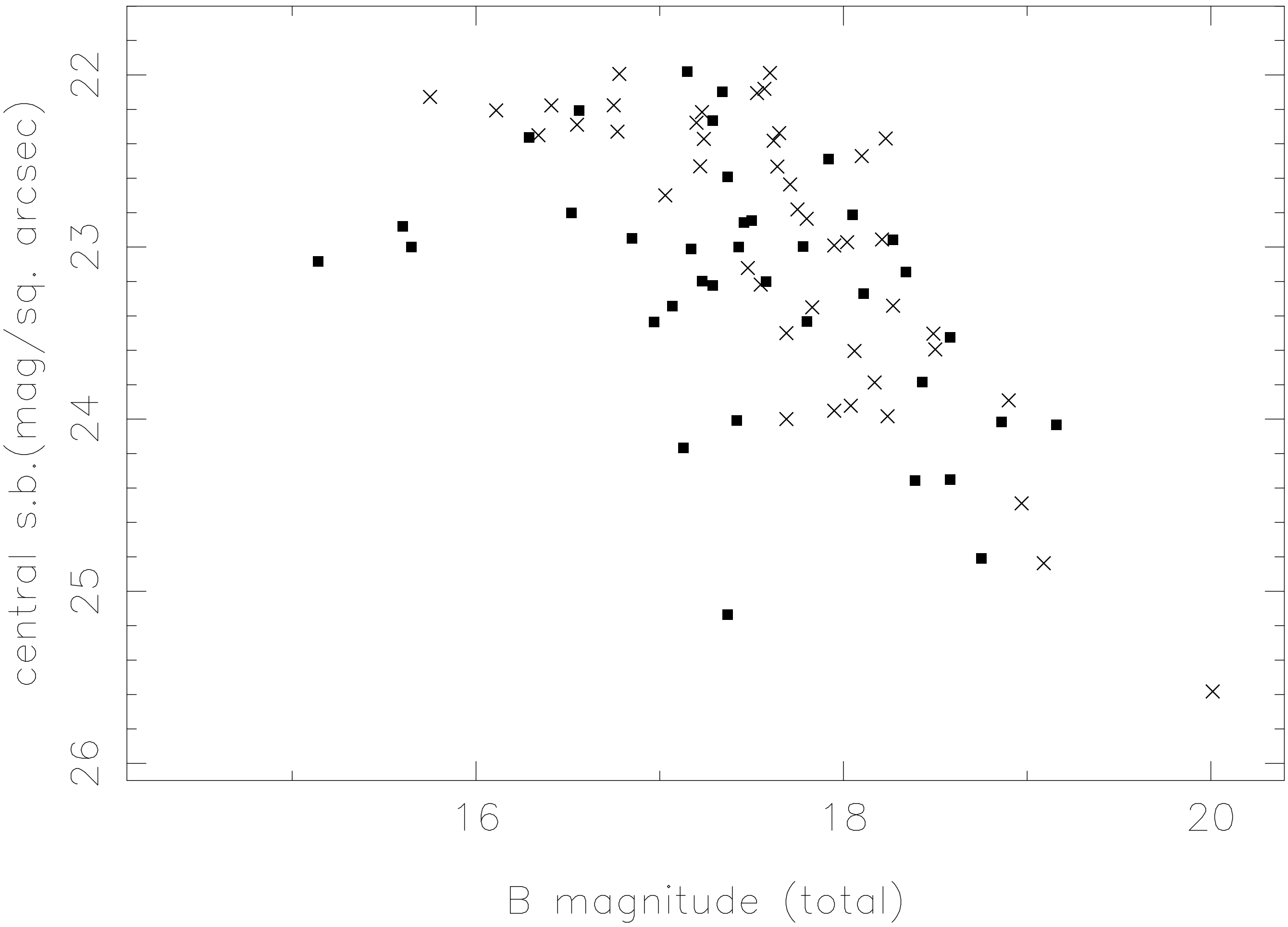
central s.b.(mag/sq. arcsec)
22
23
24
25
26
16
18
20
B magnitude (total)

Fig. 4.—

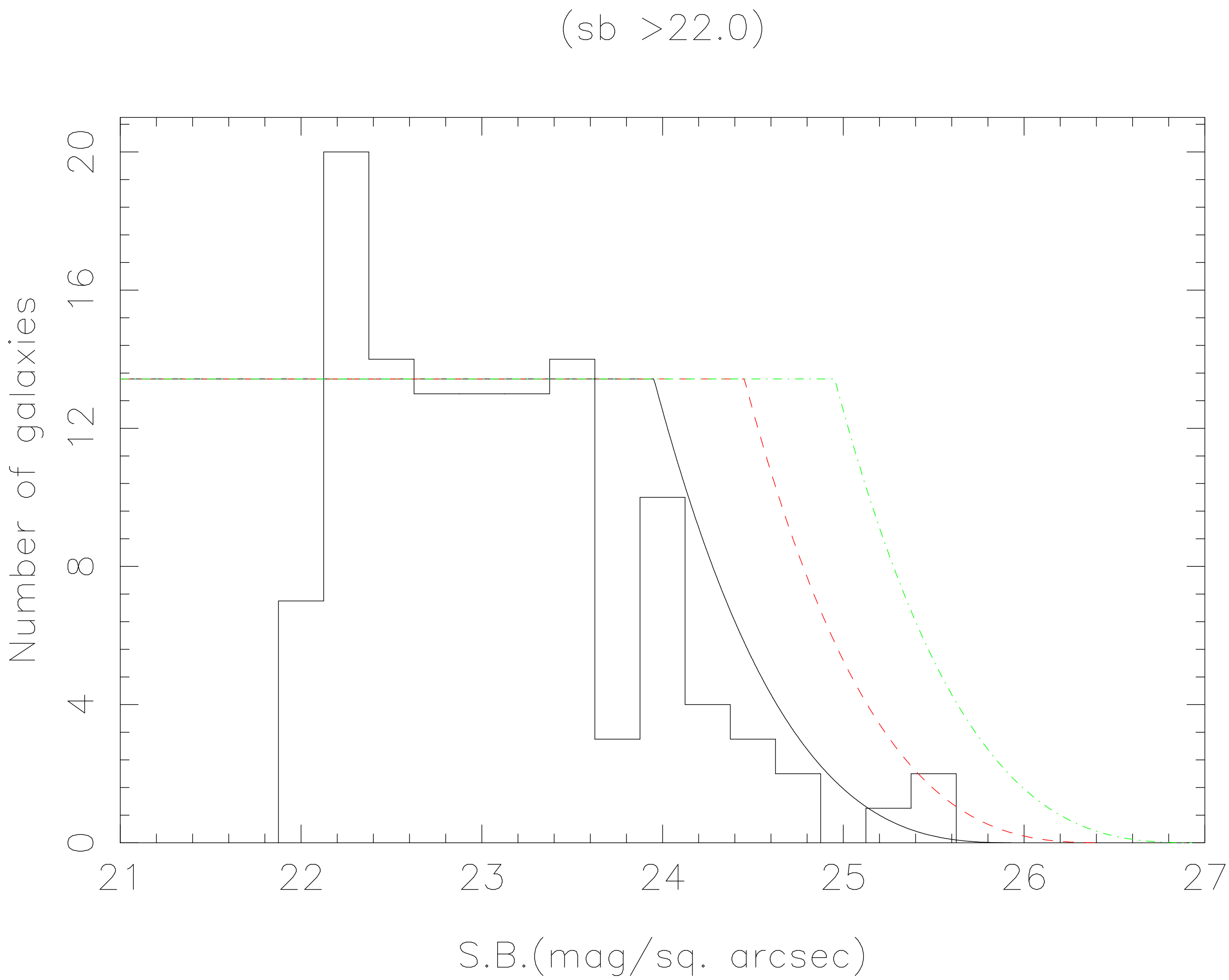

(sb >22.0)
Number of galaxies
0
4
8
12
16
20
21
22
23
24
25
26
27
S.B.(mag/sq. arcsec)

Fig. 5.—

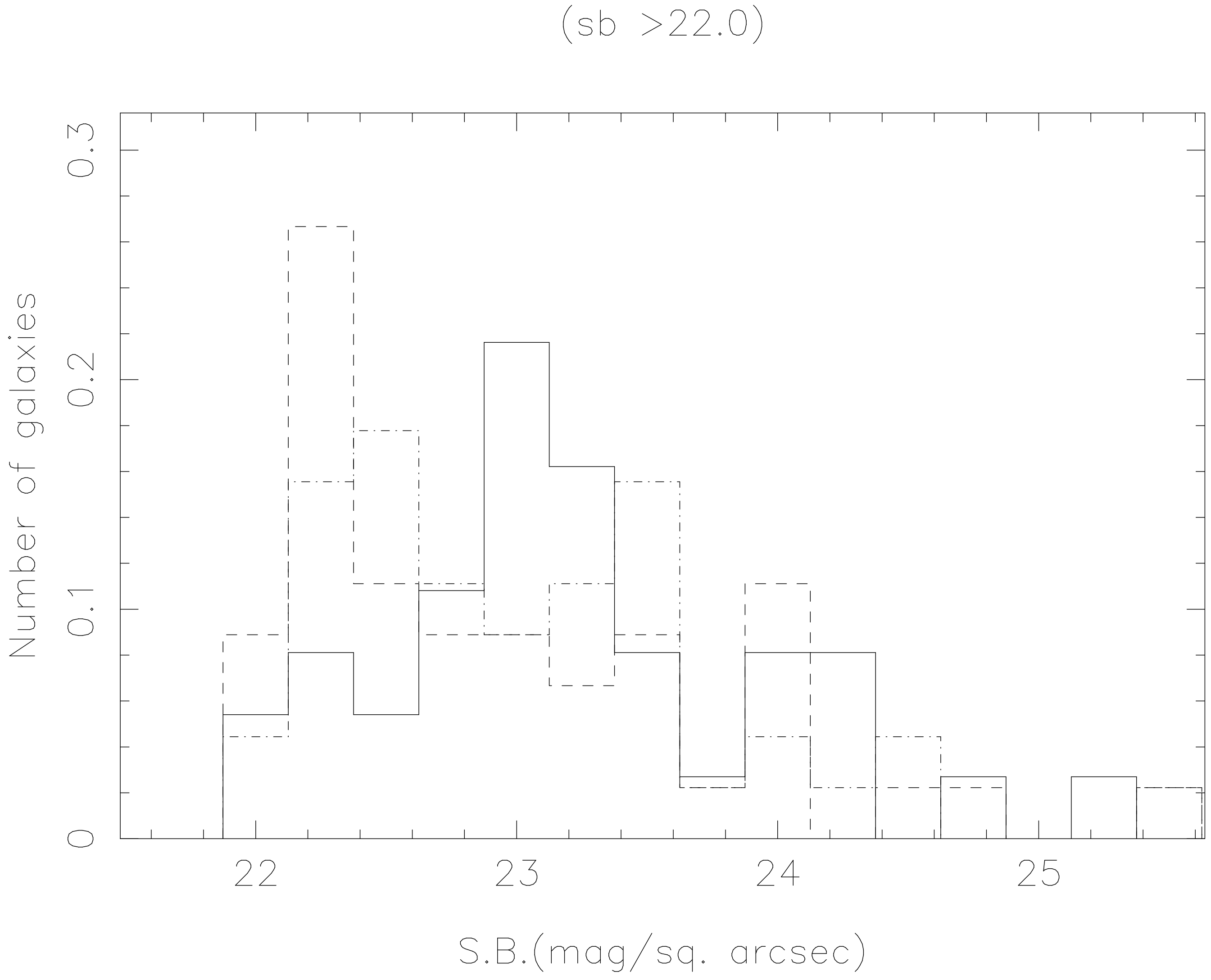

Fig. 6.—

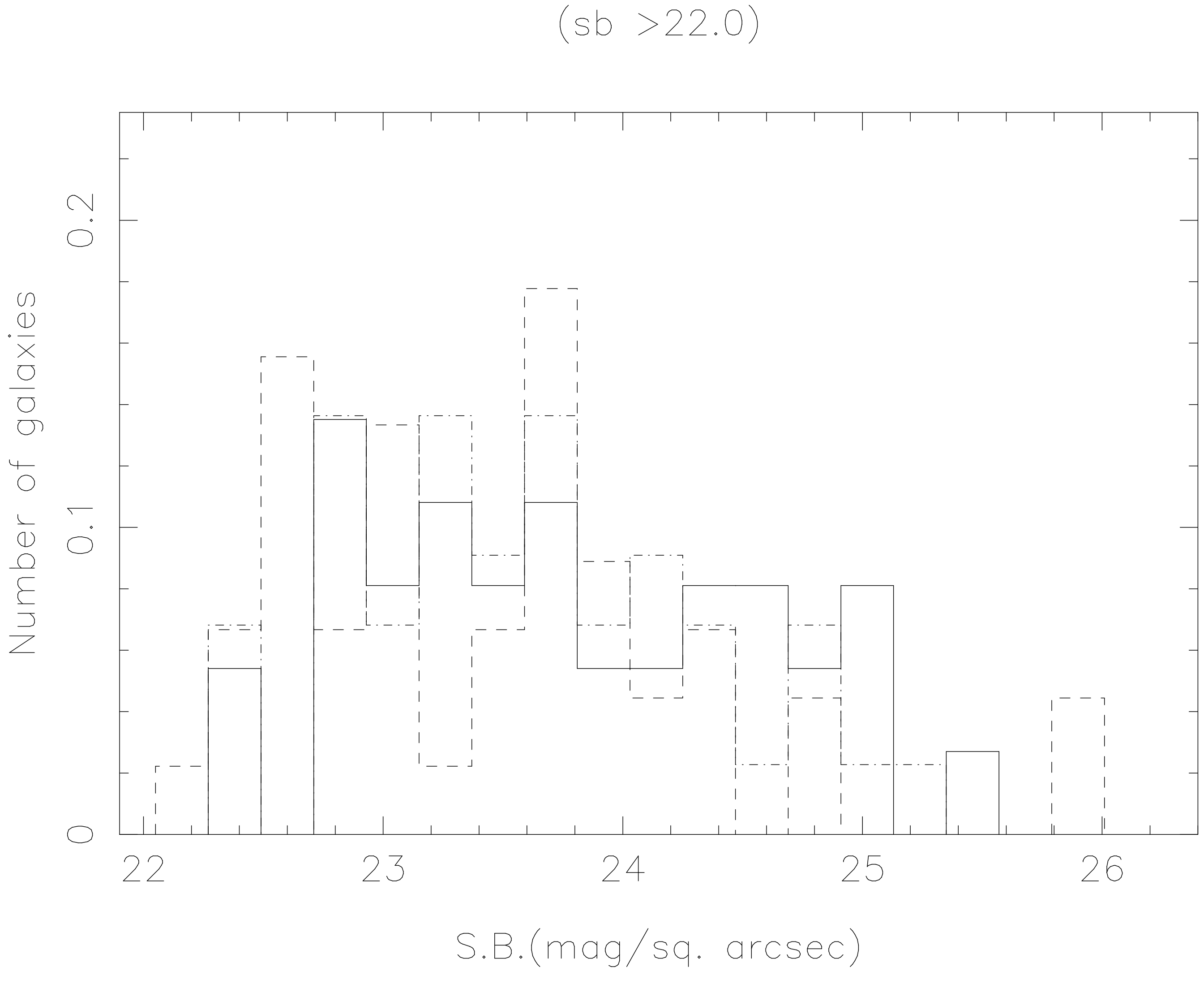

Fig. 7.—

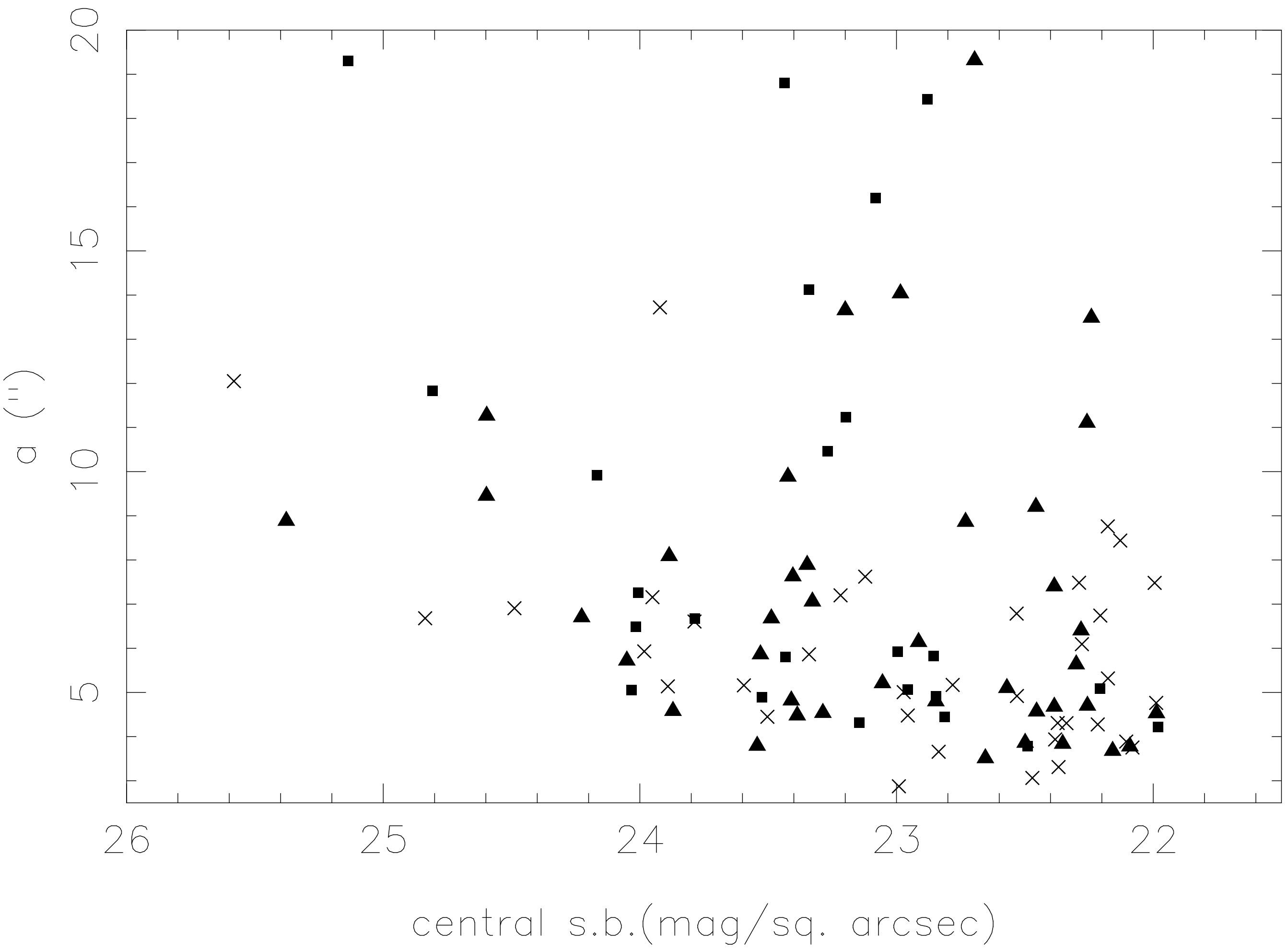

Fig. 8.—

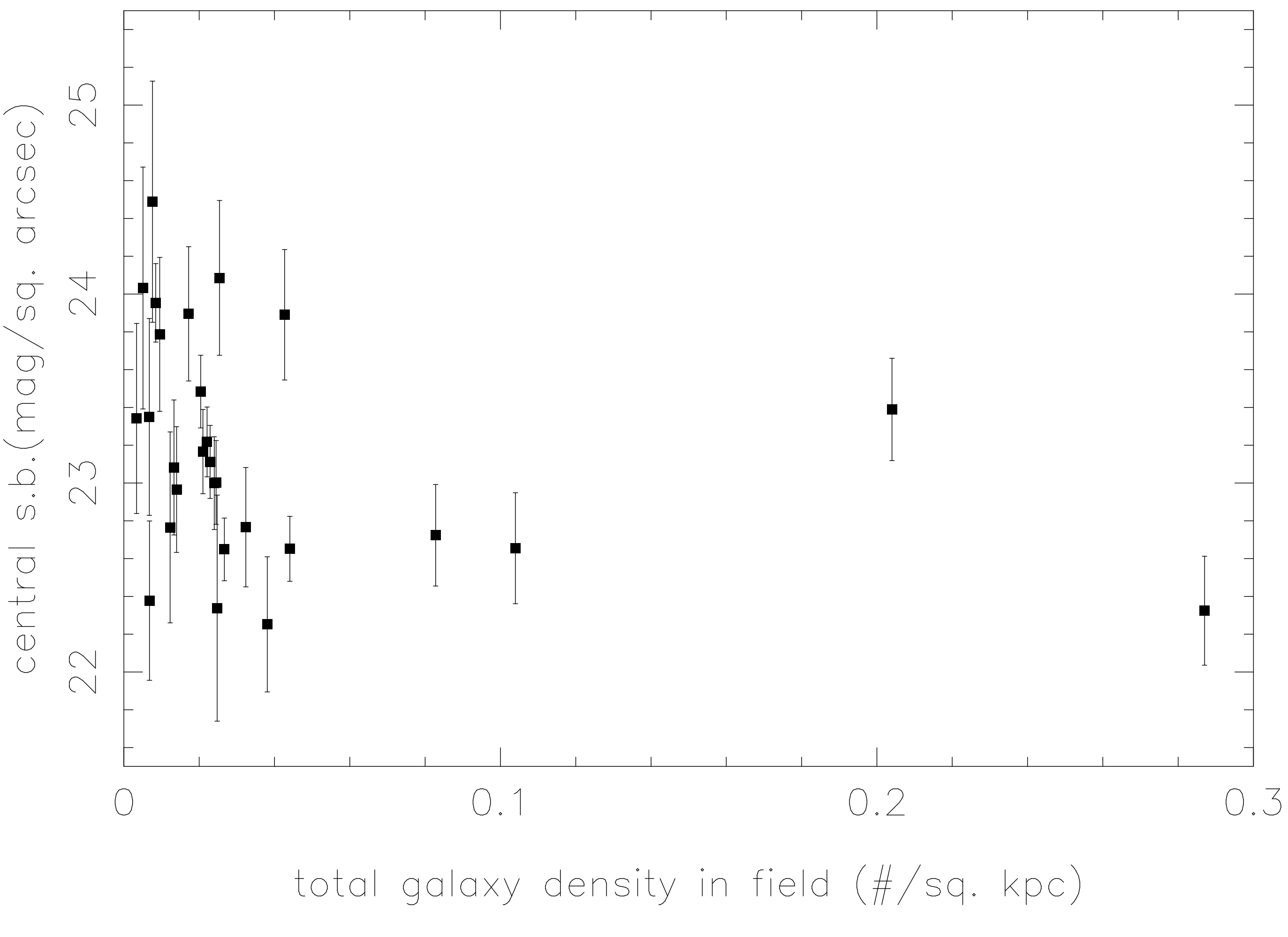

central s.b.(mag/sq. arcsec)
22
23
24
25
0
0.1
0.2
0.3
total galaxy density in field (#/sq. kpc)

Fig. 9.—

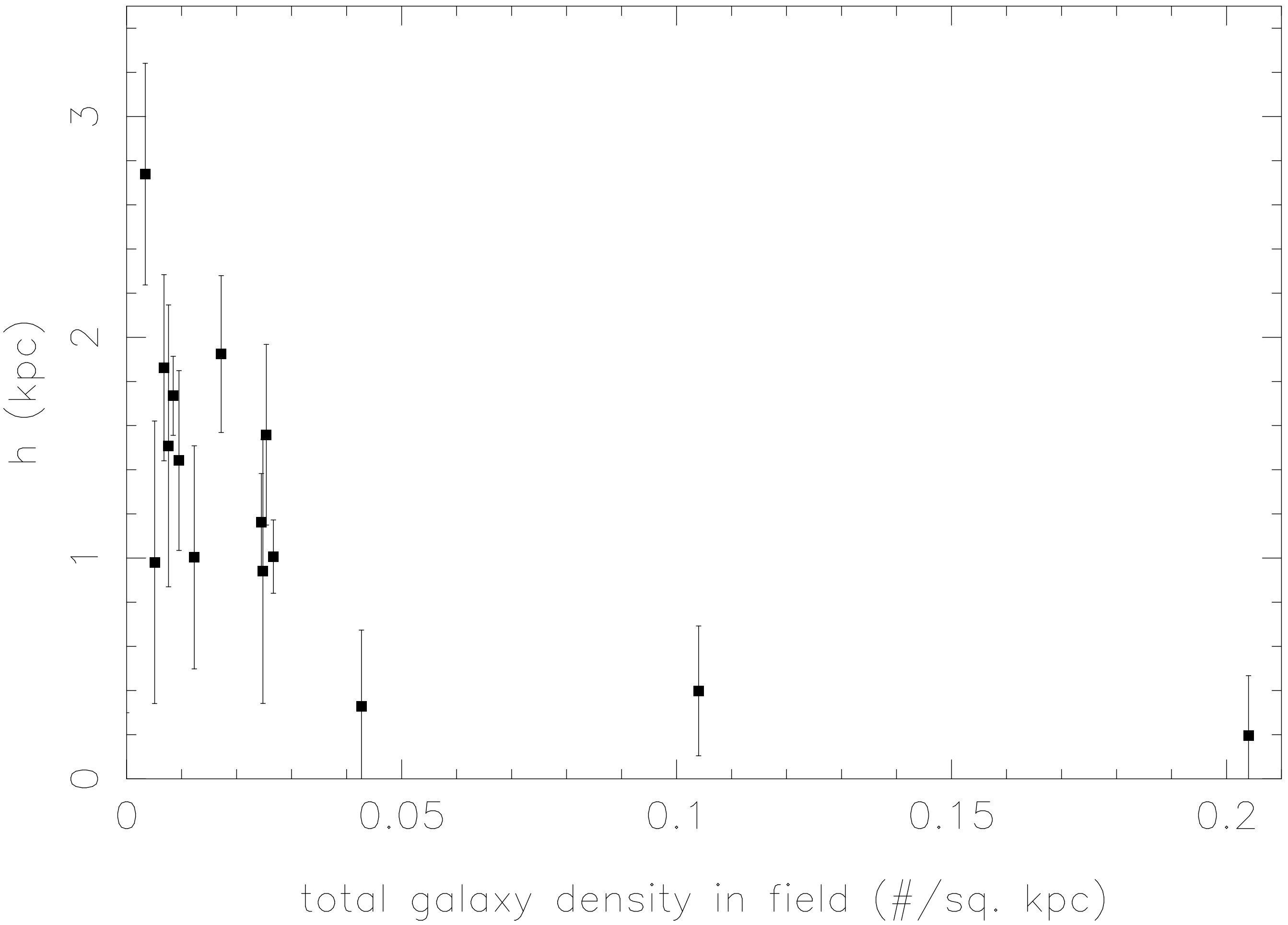

Fig. 10.—

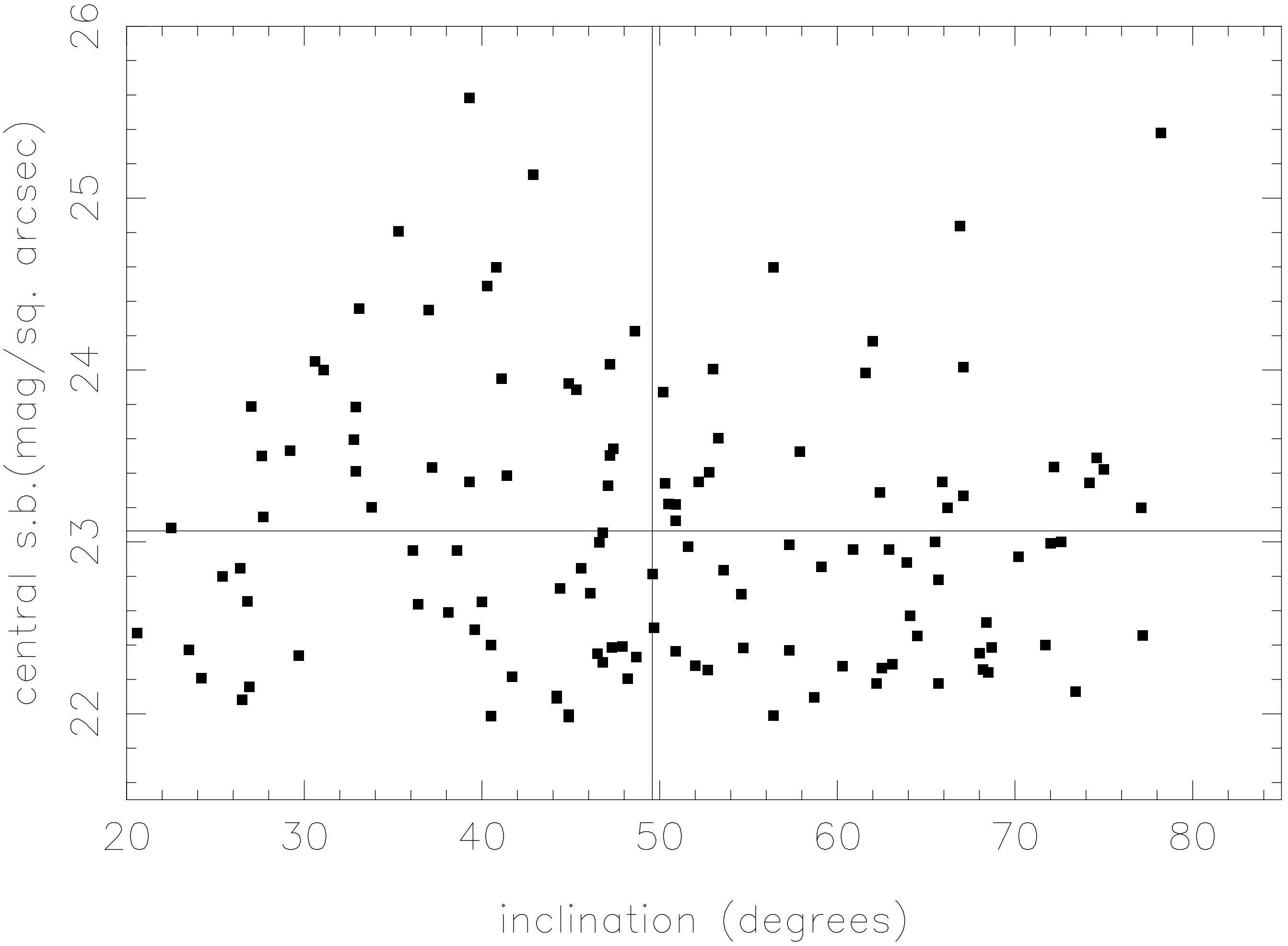
central s.b.(mag/sq. arcsec)
inclination (degrees)
20
30
40
50
60
70
80
22
23
24
25
26

Fig. 11.—

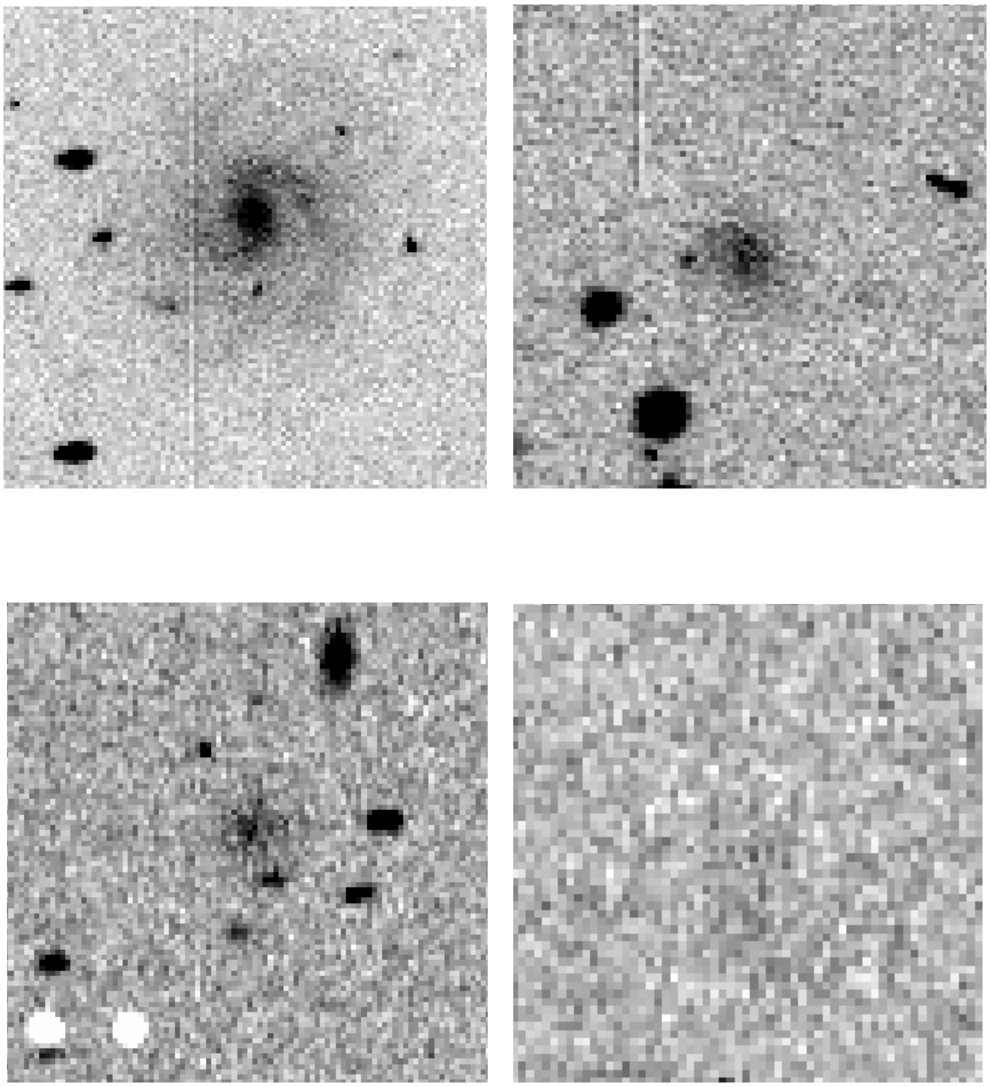

Fig. 12.—

p1-1 (b)

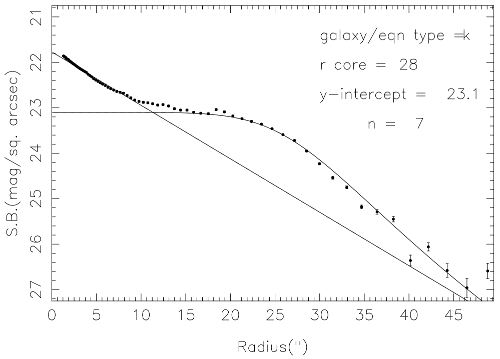

p1-4 (b)

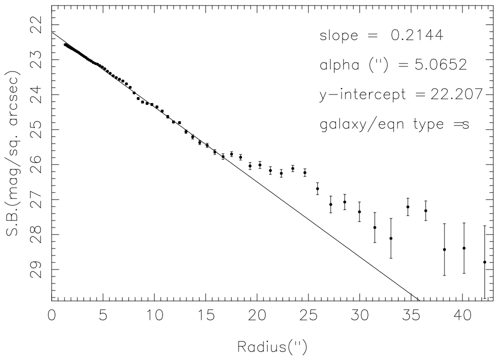

p1-7 (b)

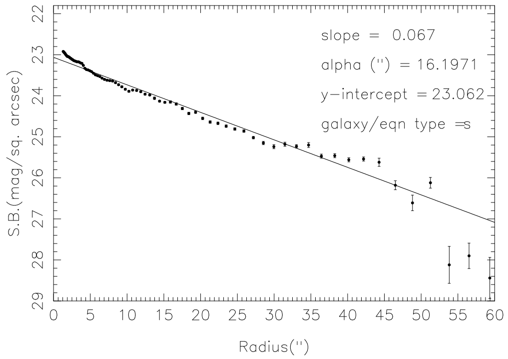

p1-2 (b)

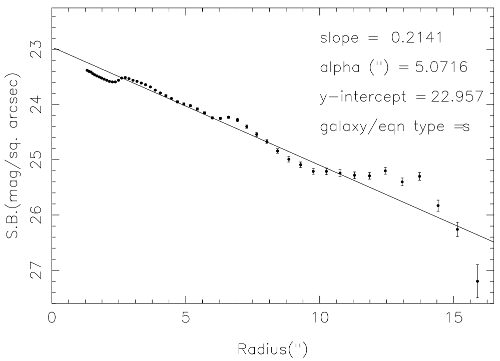

p1-5 (b)

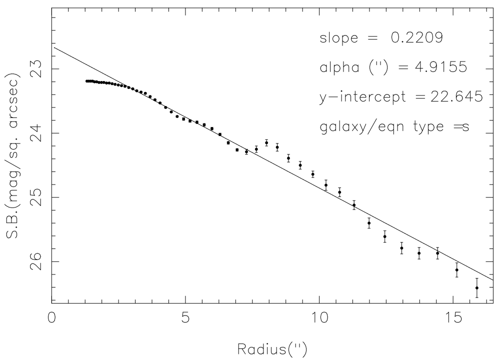

p2-1 (b)

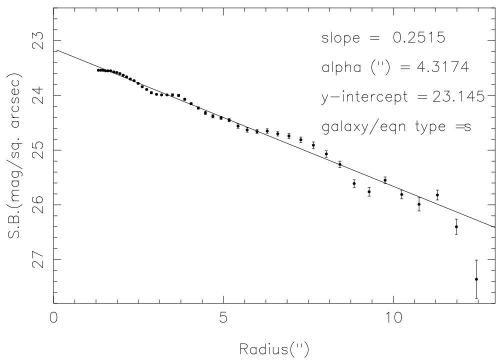

p1-3 (b)

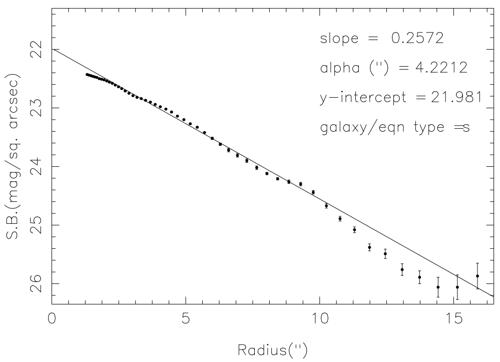

p1-6 (b)

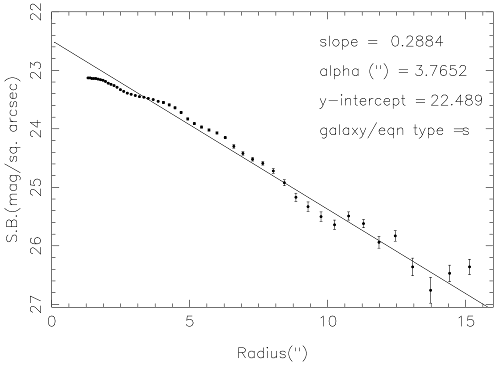

p2-2 (b)

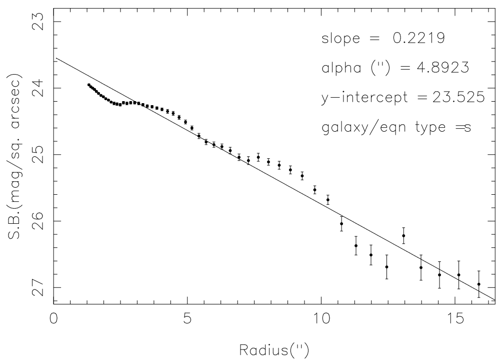

p2-3 (b)

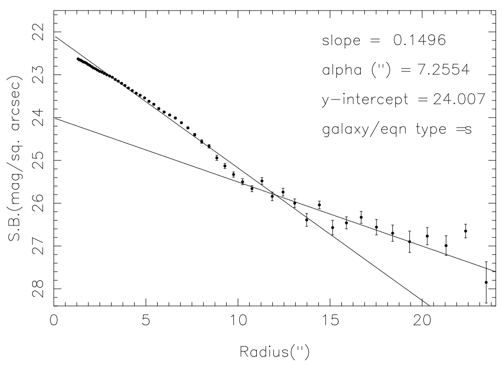

p3-2 (b)

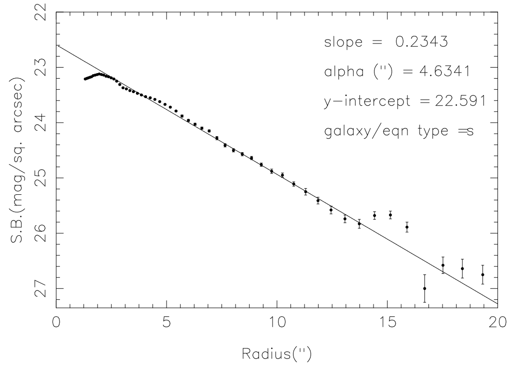

p4-1 (b)

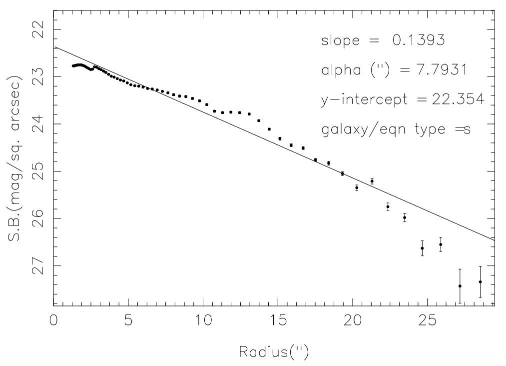

p2-4 (b)

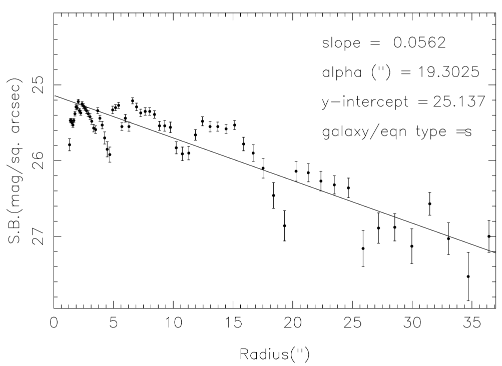

p3-3 (b)

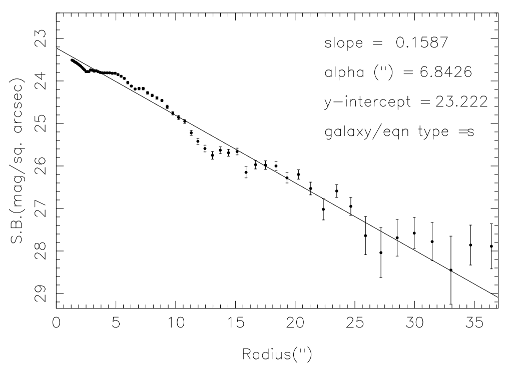

p4-2 (b)

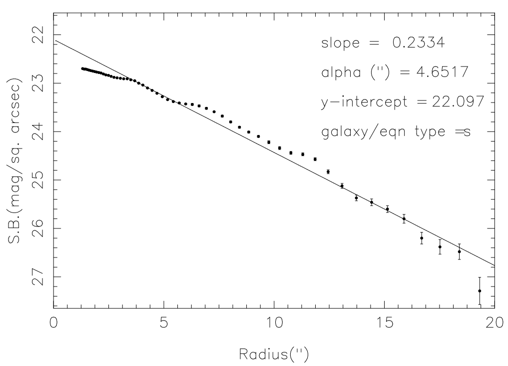

p3-1 (b)

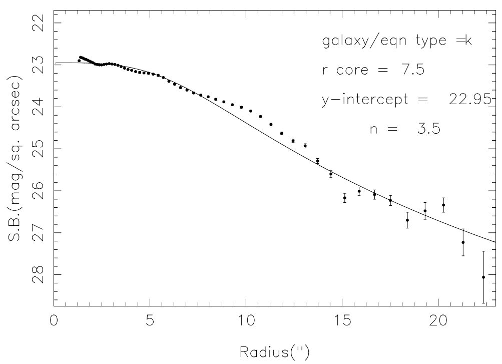

p3-4 (b)

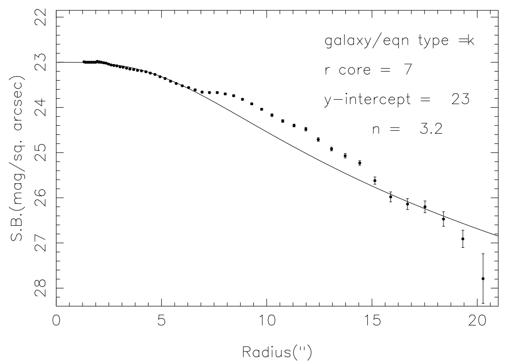

p4-3 (b)

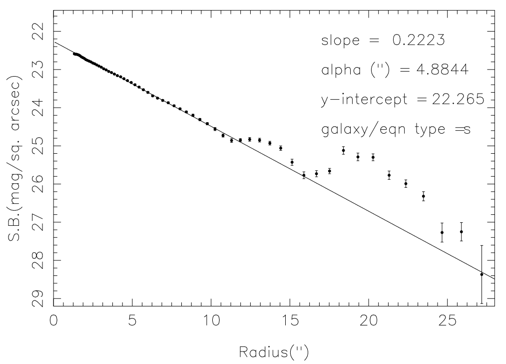

p4−4 (b)

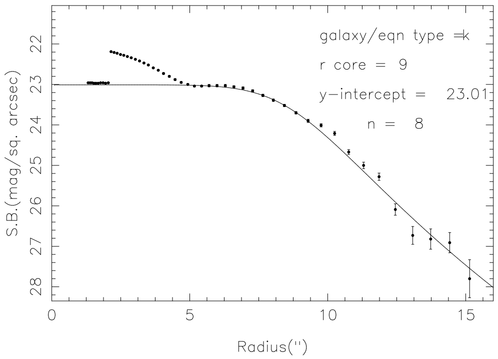

p5−3 (b)

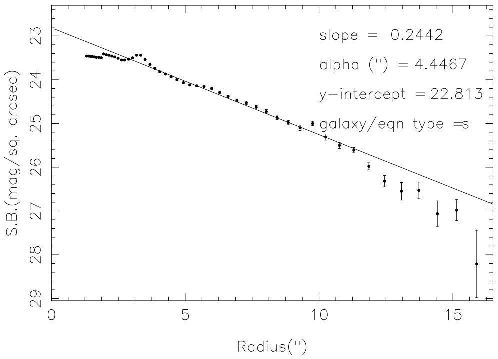

p5−6 (b)

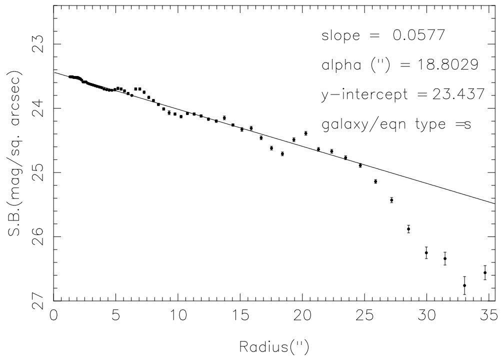

p5−1 (b)

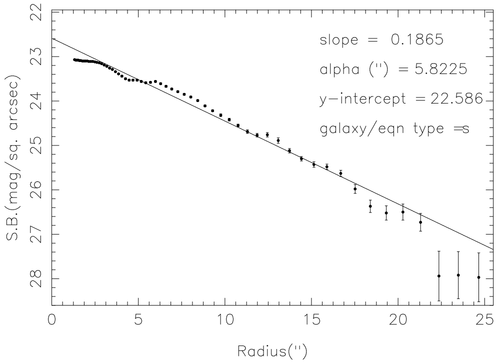

p5−4 (b)

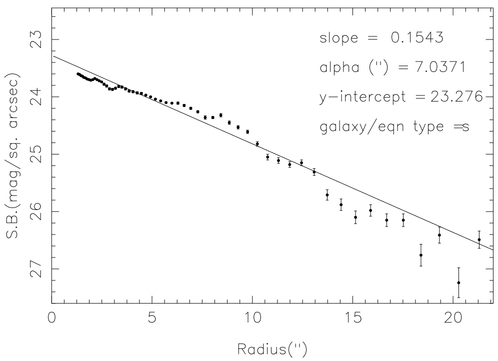

p5−7 (b)

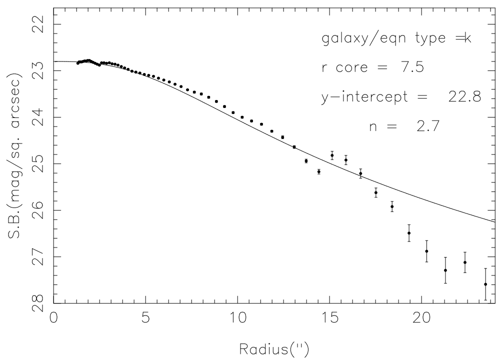

p5−2 (b)

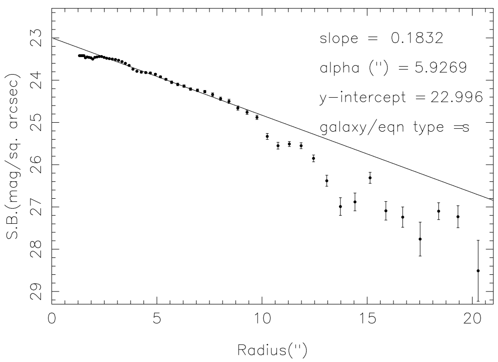

p5−5 (b)

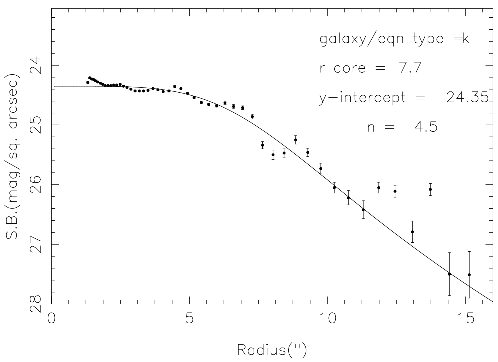

p6−1 (b)

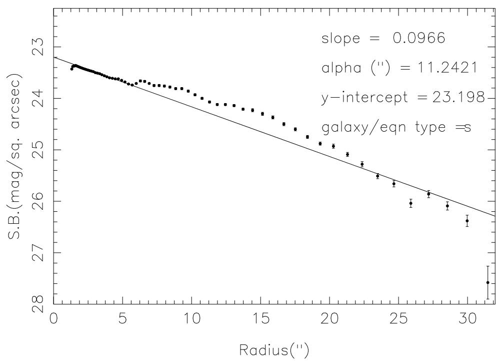

p6-2 (b)

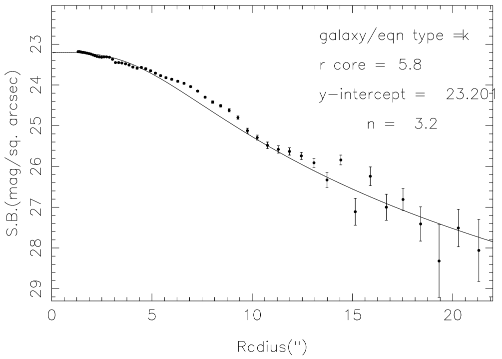

p6-5 (b)

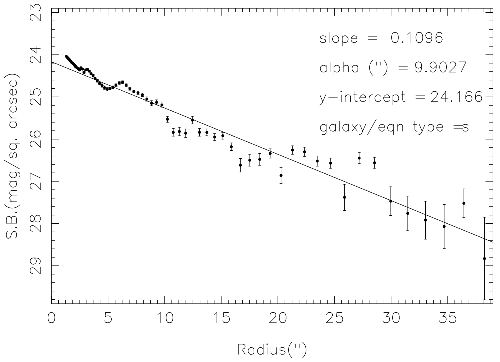

p9-1 (b)

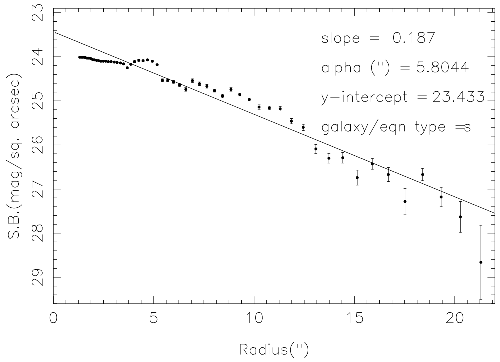

p6-3 (b)

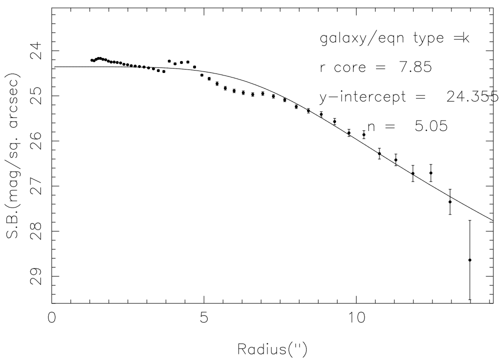

p6-6 (b)

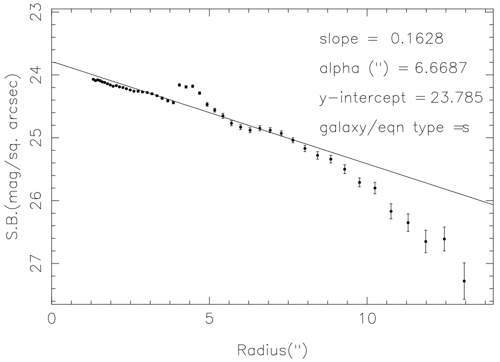

p9-3 (b)

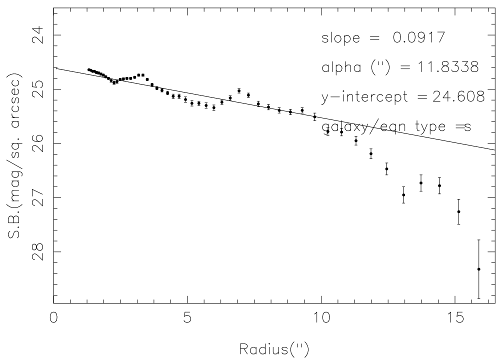

p6-4 (b)

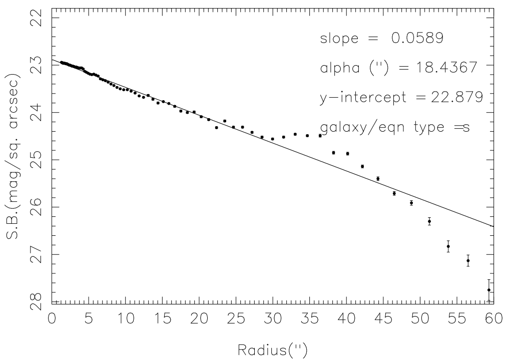

p7-1 (b)

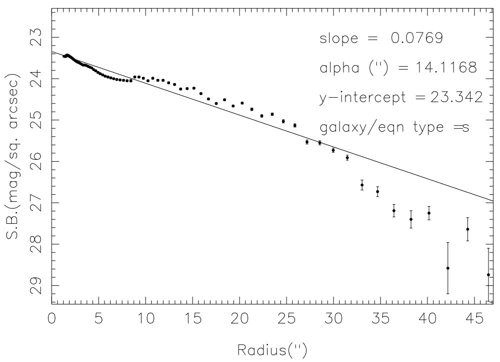

p9-4 (b)

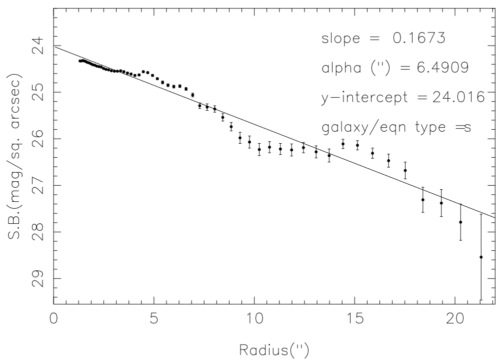

P10-1 (b)

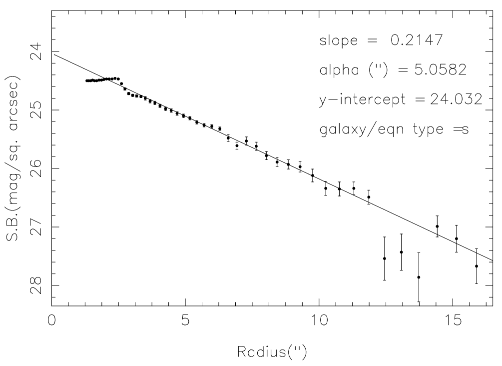

c1-3 (b)

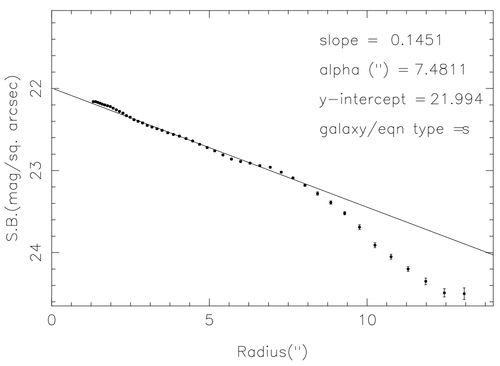

c1-6 (b)

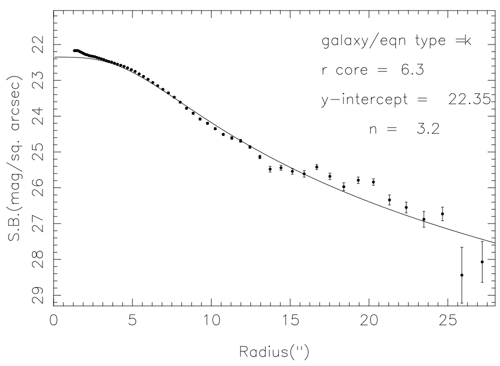

c1-1 (b)

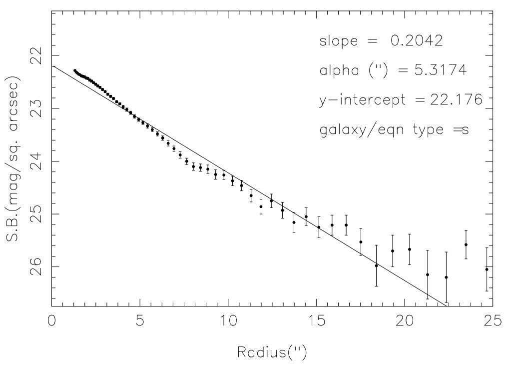

c1-4 (b)

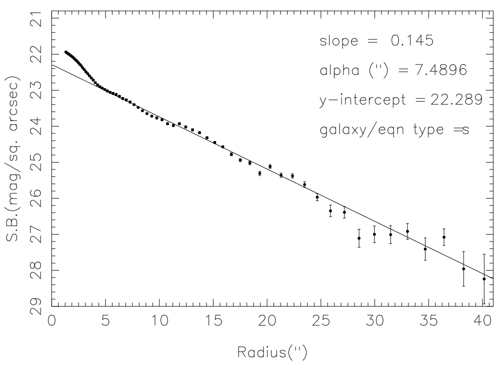

c2-1 (b)

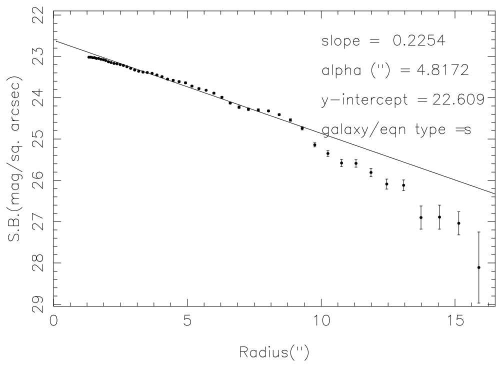

c1-2 (b)

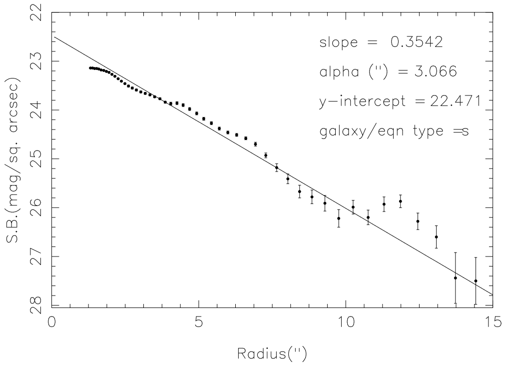

c1-5 (b)

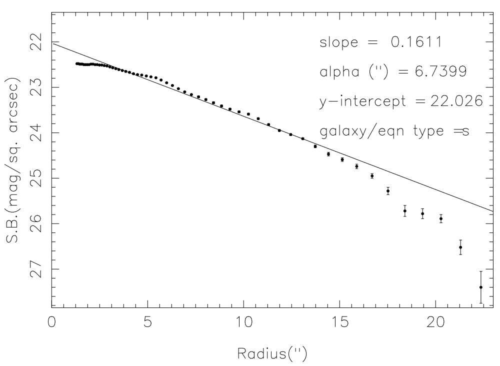

c3-1 (b)

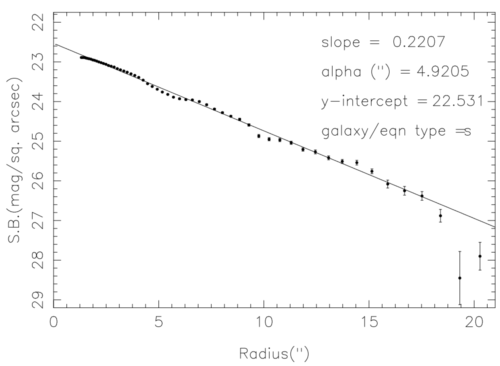

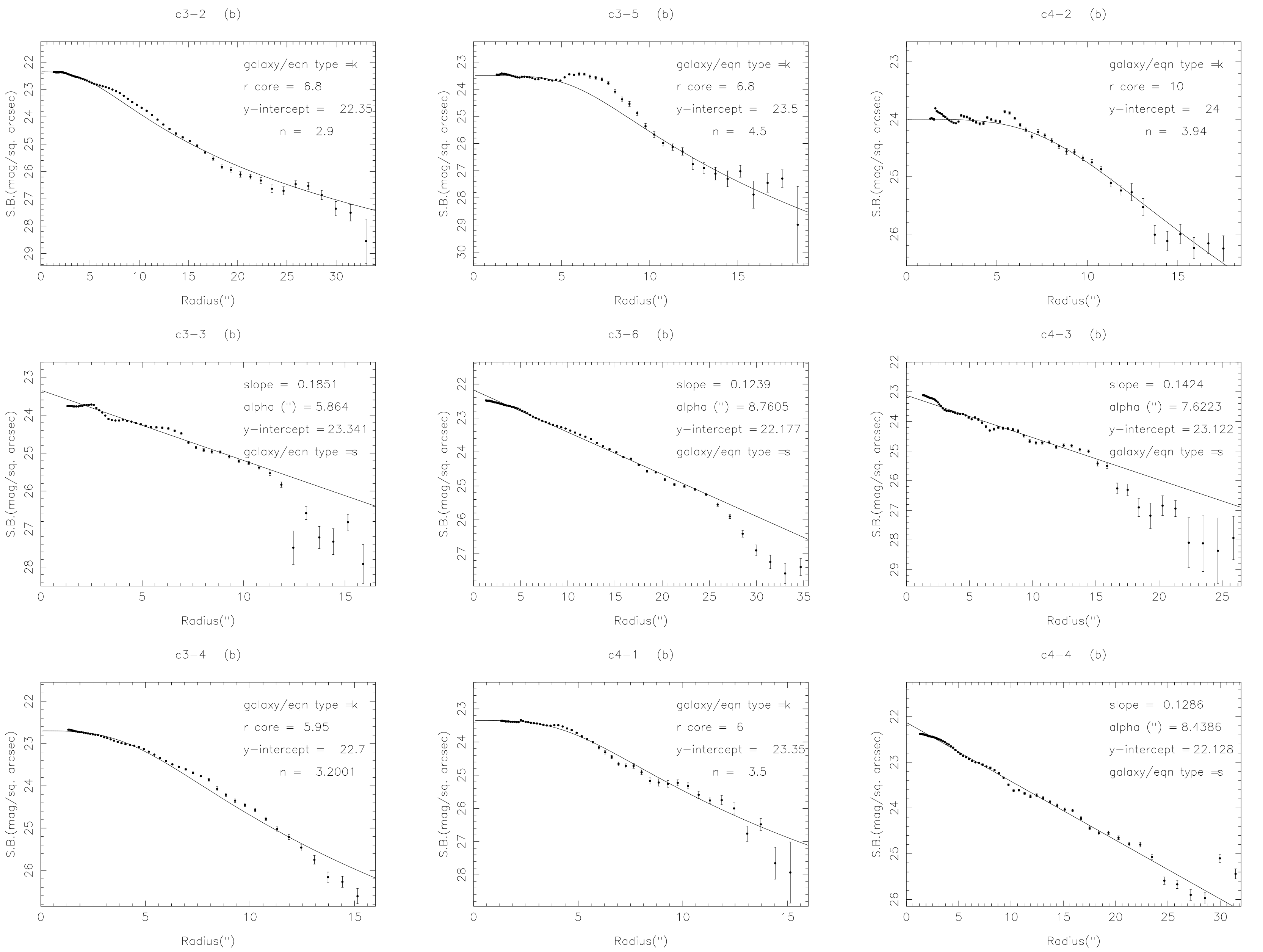
c3-2 (b)
galaxy/eqn type =k
r core = 6.8
y-intercept = 22.35
n = 2.9
c3-5 (b)
galaxy/eqn type =k
r core = 6.8
y-intercept = 23.5
n = 4.5
c4-2 (b)
galaxy/eqn type =k
r core = 10
y-intercept = 24
n = 3.94
c3-3 (b)
slope = 0.1851
alpha ('') = 5.864
y-intercept = 23.341
galaxy/eqn type =s
c3-6 (b)
slope = 0.1239
alpha ('') = 8.7605
y-intercept = 22.177
galaxy/eqn type =s
c4-3 (b)
slope = 0.1424
alpha ('') = 7.6223
y-intercept = 23.122
galaxy/eqn type =s
c3-4 (b)
galaxy/eqn type =k
r core = 5.95
y-intercept = 22.7
n = 3.2001
c4-1 (b)
galaxy/eqn type =k
r core = 6
y-intercept = 23.35
n = 3.5
c4-4 (b)
slope = 0.1286
alpha ('') = 8.4386
y-intercept = 22.128
galaxy/eqn type =s
S.B.(mag/sq. arcsec)
Radius('')

c4-5 (b)

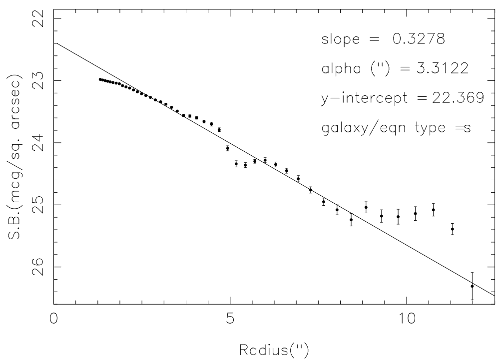

c4-7 (b)

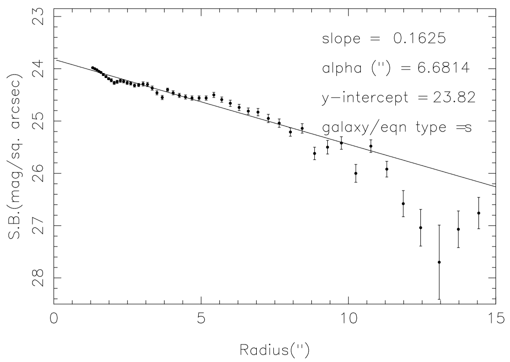

c4-8 (b)

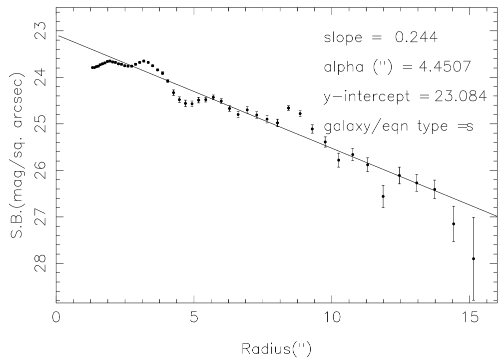

c5-1 (b)

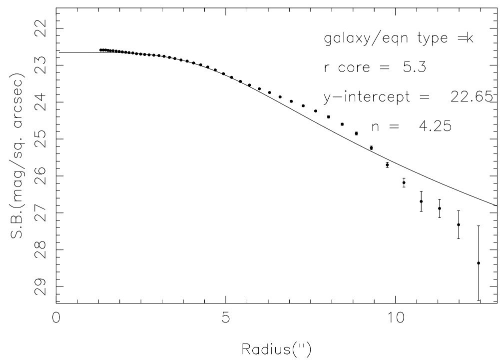

c5-2 (b)

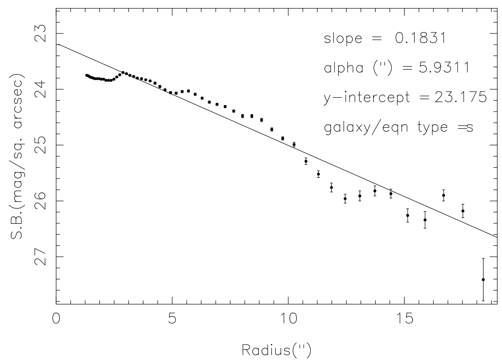

c5-3 (b)

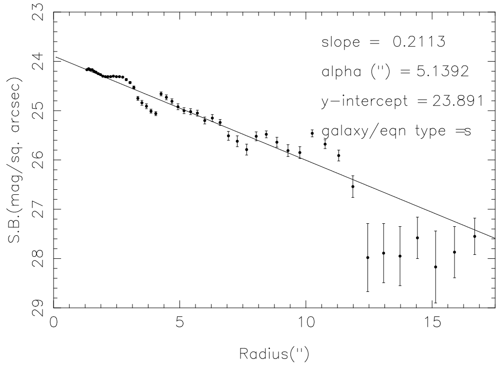

c5-4 (b)

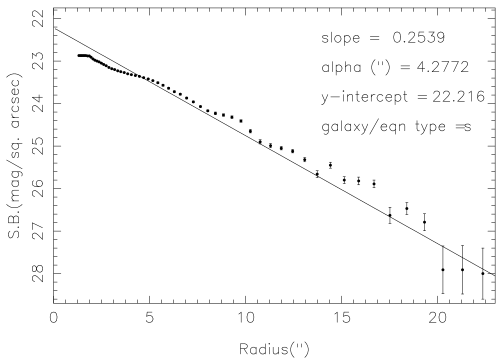

c5-5 (b)

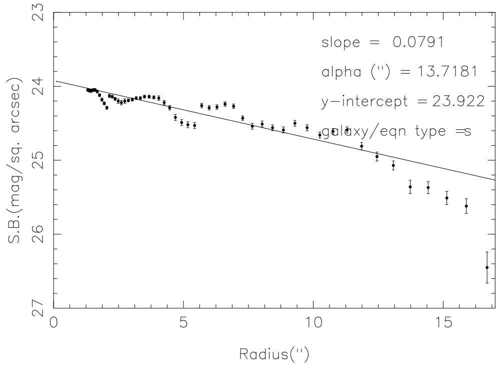

c6-1 (b)

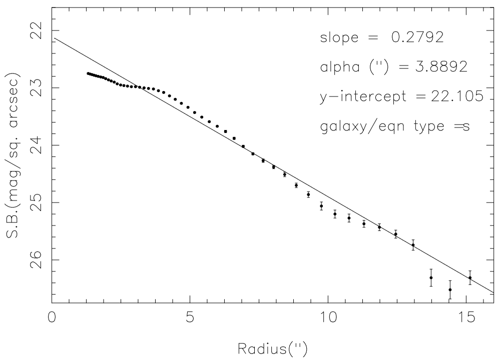

c6-4 (b)

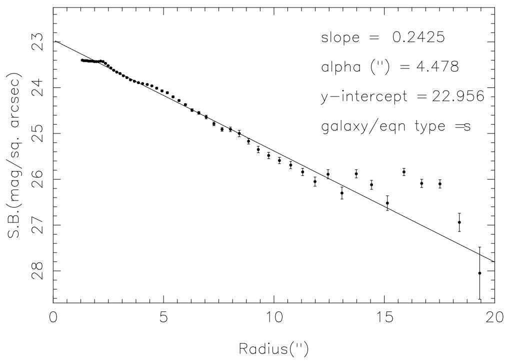

c8-1 (b)

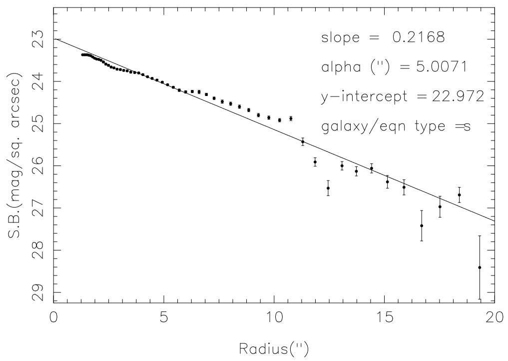

c6-2 (b)

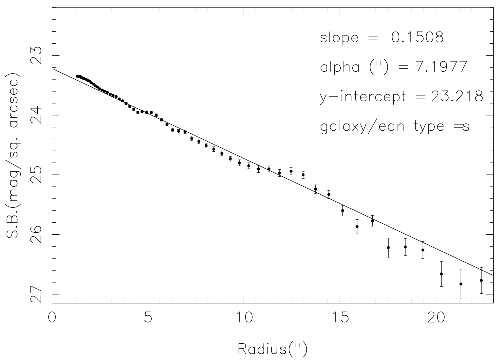

c6-5 (b)

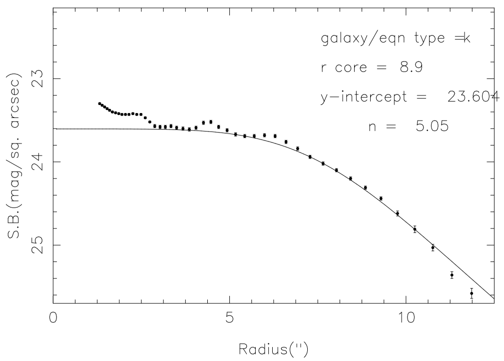

c8-2 (b)

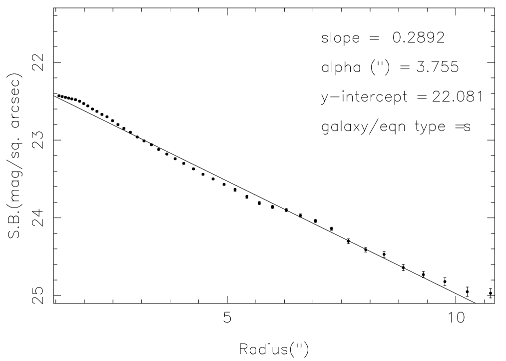

c6-3 (b)

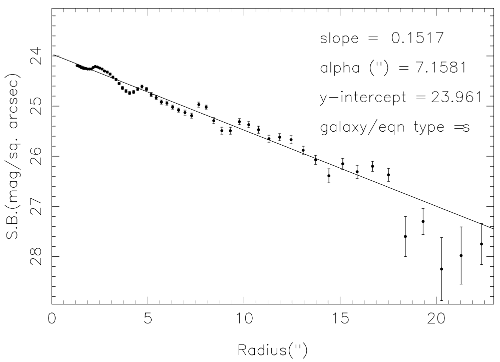

c6-6 (b)

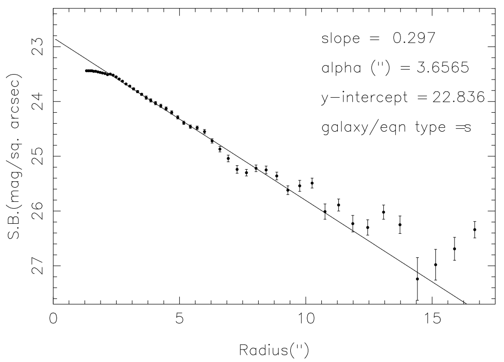

c8-3 (b)

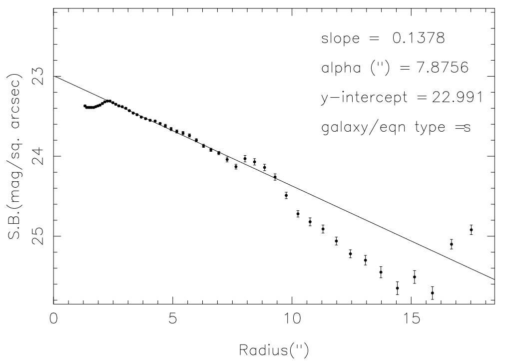

c8-4 (b)

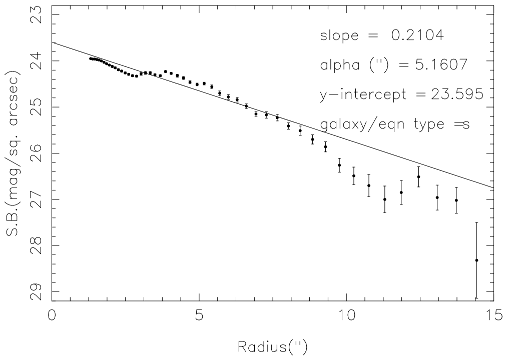

c8-8 (b)

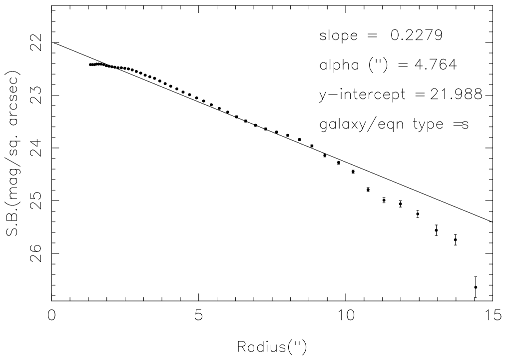

c11-1 (b)

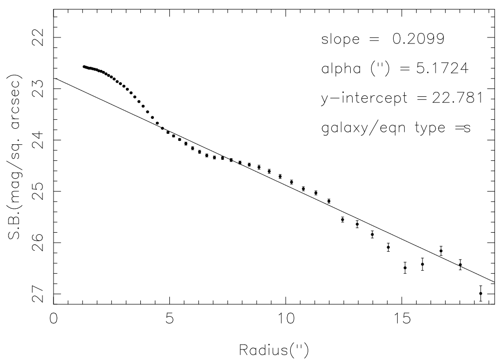

c8-5 (b)

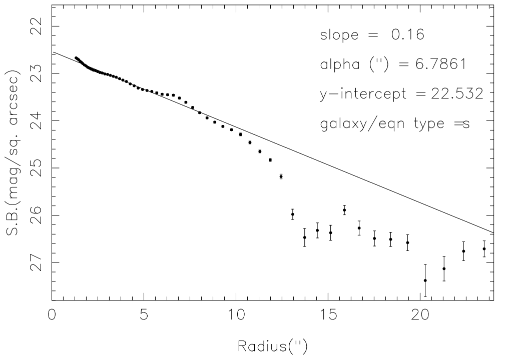

c9-1 (b)

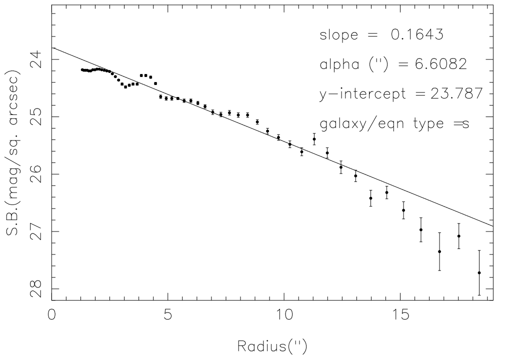

c11-3 (b)

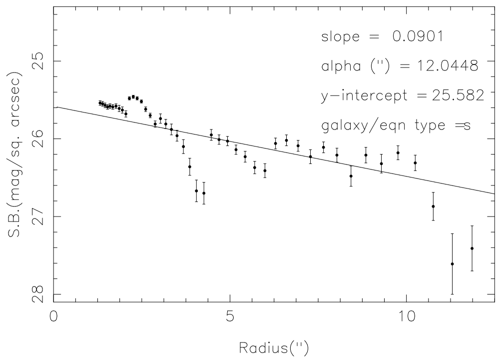

c8-6 (b)

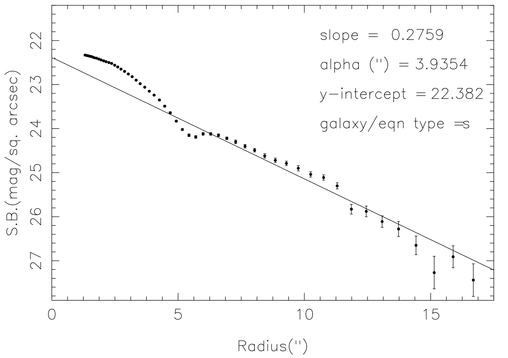

c10-1 (b)

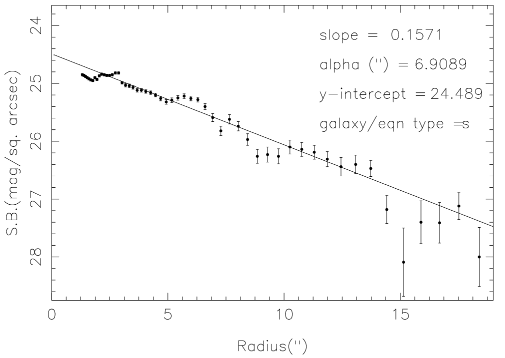

c11-4 (b)

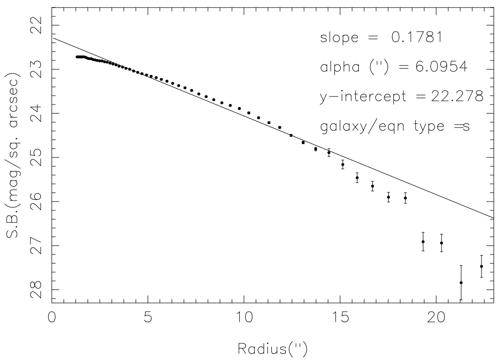

n1-2 (b)

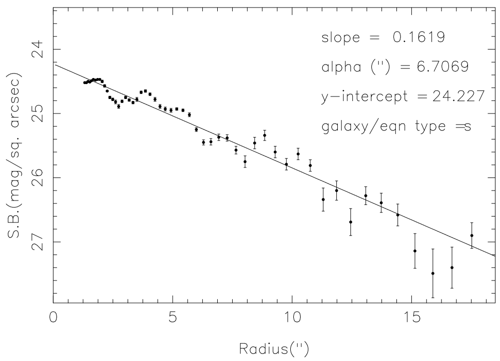

n2-2 (b)

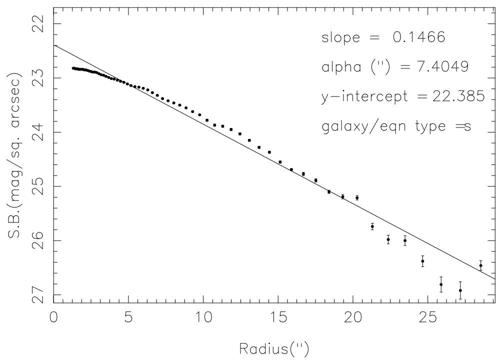

c11-5 (b)

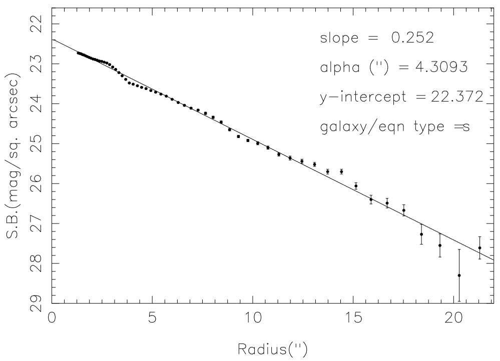

n1-3 (b)

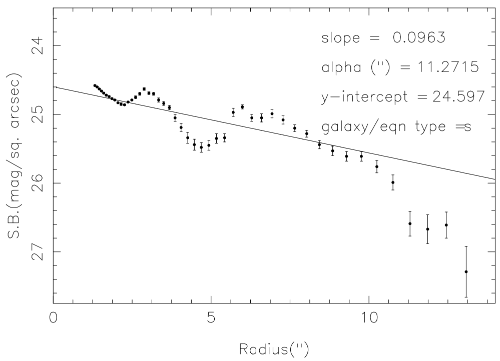

n2-3 (b)

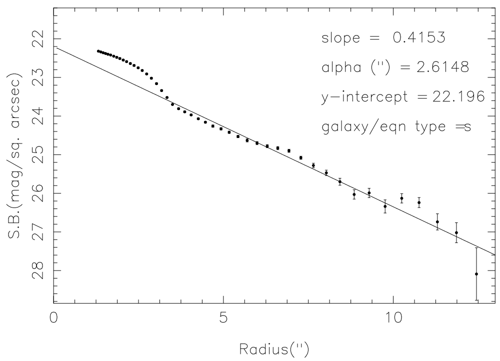

n1-1 (b)

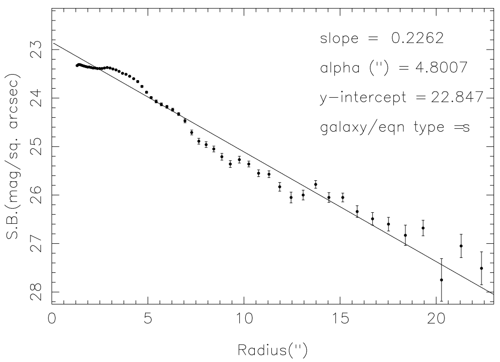

n2-1 (b)

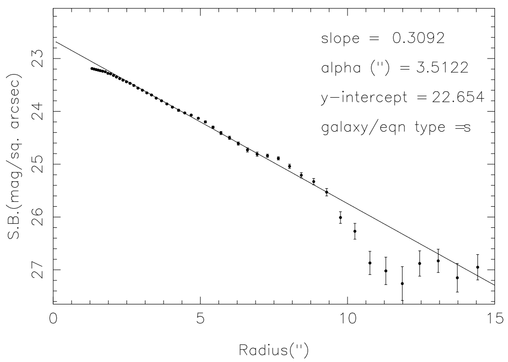

n2-4 (b)

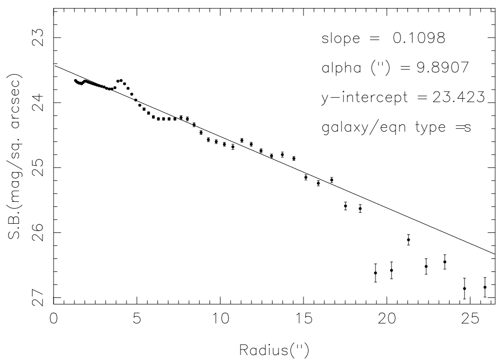

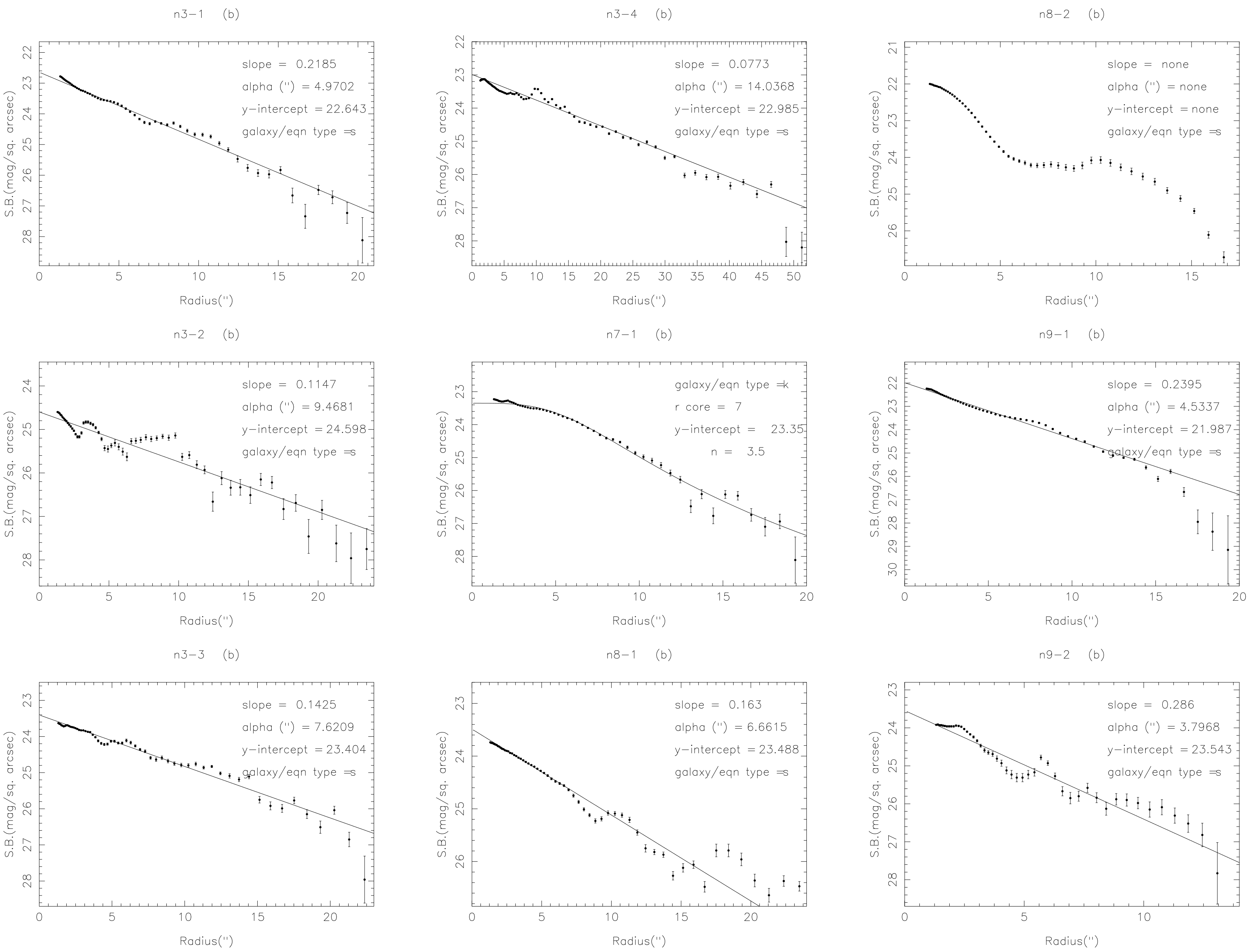

n3-1 (b)
slope = 0.2185
alpha ('') = 4.9702
y-intercept = 22.643
galaxy/eqn type =s
S.B.(mag/sq. arcsec)
Radius('')
n3-4 (b)
slope = 0.0773
alpha ('') = 14.0368
y-intercept = 22.985
galaxy/eqn type =s
S.B.(mag/sq. arcsec)
Radius('')
n8-2 (b)
slope = none
alpha ('') = none
y-intercept = none
galaxy/eqn type =s
S.B.(mag/sq. arcsec)
Radius('')
n3-2 (b)
slope = 0.1147
alpha ('') = 9.4681
y-intercept = 24.598
galaxy/eqn type =s
S.B.(mag/sq. arcsec)
Radius('')
n7-1 (b)
galaxy/eqn type =k
r core = 7
y-intercept = 23.35
n = 3.5
S.B.(mag/sq. arcsec)
Radius('')
n9-1 (b)
slope = 0.2395
alpha ('') = 4.5337
y-intercept = 21.987
galaxy/eqn type =s
S.B.(mag/sq. arcsec)
Radius('')
n3-3 (b)
slope = 0.1425
alpha ('') = 7.6209
y-intercept = 23.404
galaxy/eqn type =s
S.B.(mag/sq. arcsec)
Radius('')
n8-1 (b)
slope = 0.163
alpha ('') = 6.6615
y-intercept = 23.488
galaxy/eqn type =s
S.B.(mag/sq. arcsec)
Radius('')
n9-2 (b)
slope = 0.286
alpha ('') = 3.7968
y-intercept = 23.543
galaxy/eqn type =s
S.B.(mag/sq. arcsec)
Radius('')

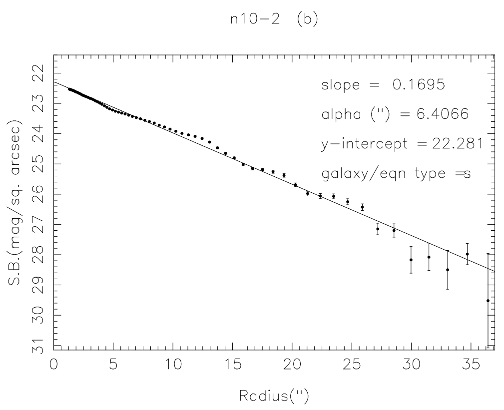
n10-2 (b)
slope = 0.1695
alpha ('') = 6.4066
y-intercept = 22.281
galaxy/eqn type =s
S.B.(mag/sq. arcsec)
Radius('')

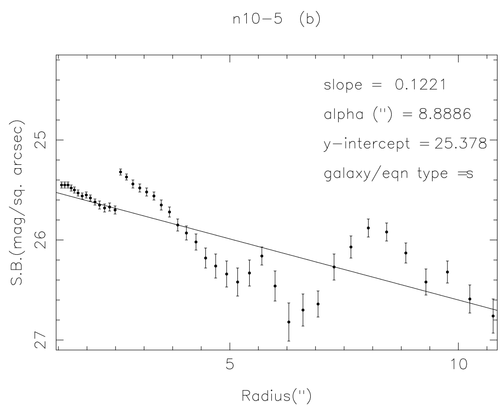
n10-5 (b)
slope = 0.1221
alpha ('') = 8.8886
y-intercept = 25.378
galaxy/eqn type =s
S.B.(mag/sq. arcsec)
Radius('')

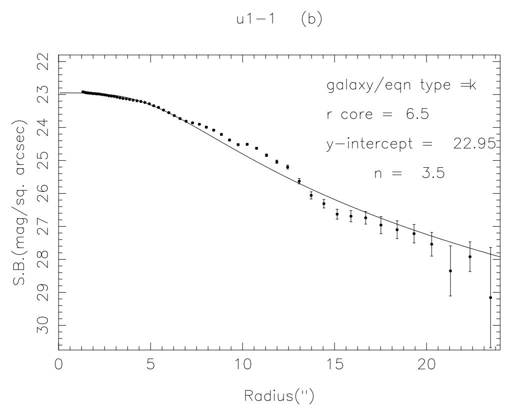
u1-1 (b)
galaxy/eqn type =k
r core = 6.5
y-intercept = 22.95
n = 3.5
S.B.(mag/sq. arcsec)
Radius('')

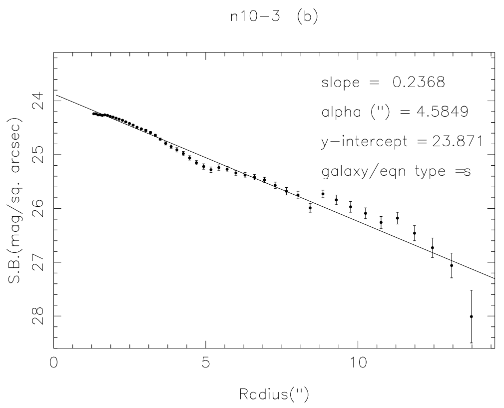
n10-3 (b)
slope = 0.2368
alpha ('') = 4.5849
y-intercept = 23.871
galaxy/eqn type =s
S.B.(mag/sq. arcsec)
Radius('')

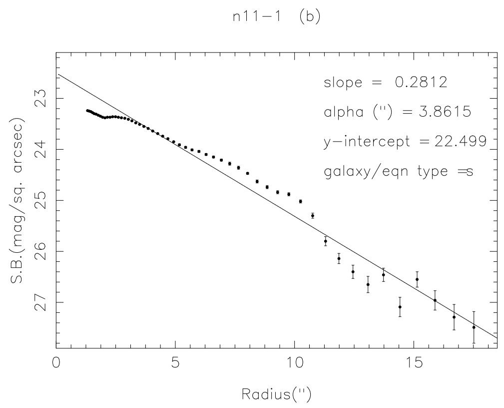
n11-1 (b)
slope = 0.2812
alpha ('') = 3.8615
y-intercept = 22.499
galaxy/eqn type =s
S.B.(mag/sq. arcsec)
Radius('')

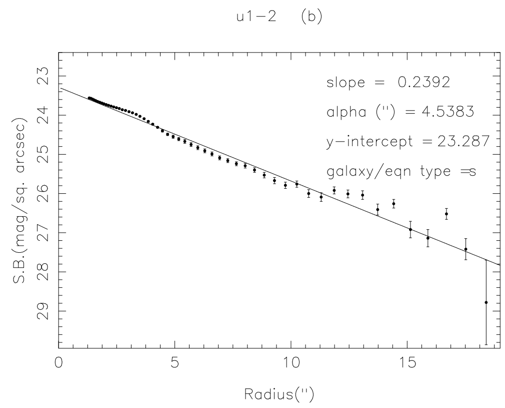
u1-2 (b)
slope = 0.2392
alpha ('') = 4.5383
y-intercept = 23.287
galaxy/eqn type =s
S.B.(mag/sq. arcsec)
Radius('')

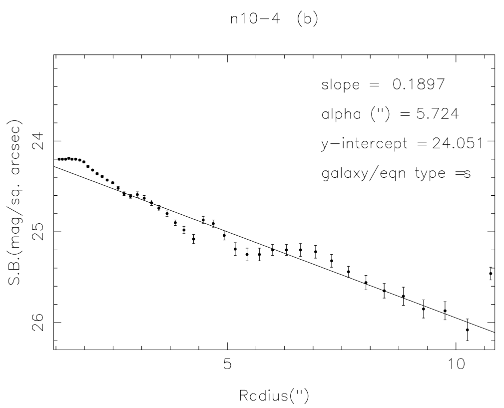
n10-4 (b)
slope = 0.1897
alpha ('') = 5.724
y-intercept = 24.051
galaxy/eqn type =s
S.B.(mag/sq. arcsec)
Radius('')

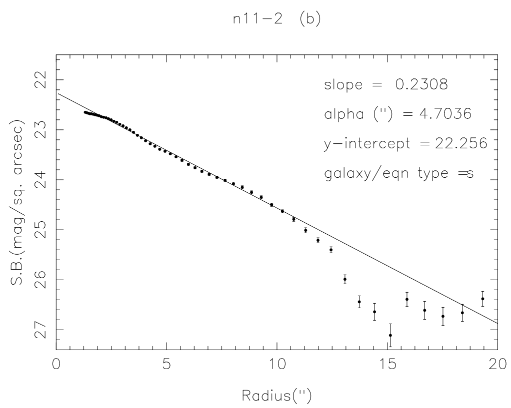
n11-2 (b)
slope = 0.2308
alpha ('') = 4.7036
y-intercept = 22.256
galaxy/eqn type =s
S.B.(mag/sq. arcsec)
Radius('')

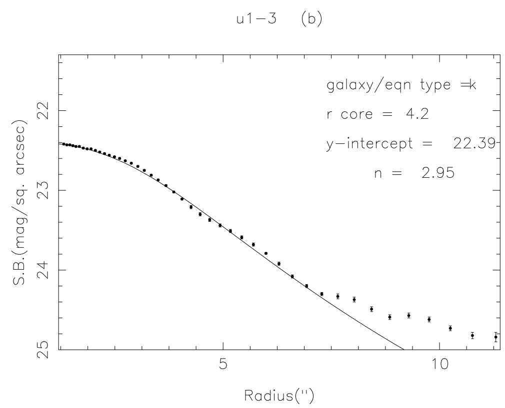
u1-3 (b)
galaxy/eqn type =k
r core = 4.2
y-intercept = 22.39
n = 2.95
S.B.(mag/sq. arcsec)
Radius('')

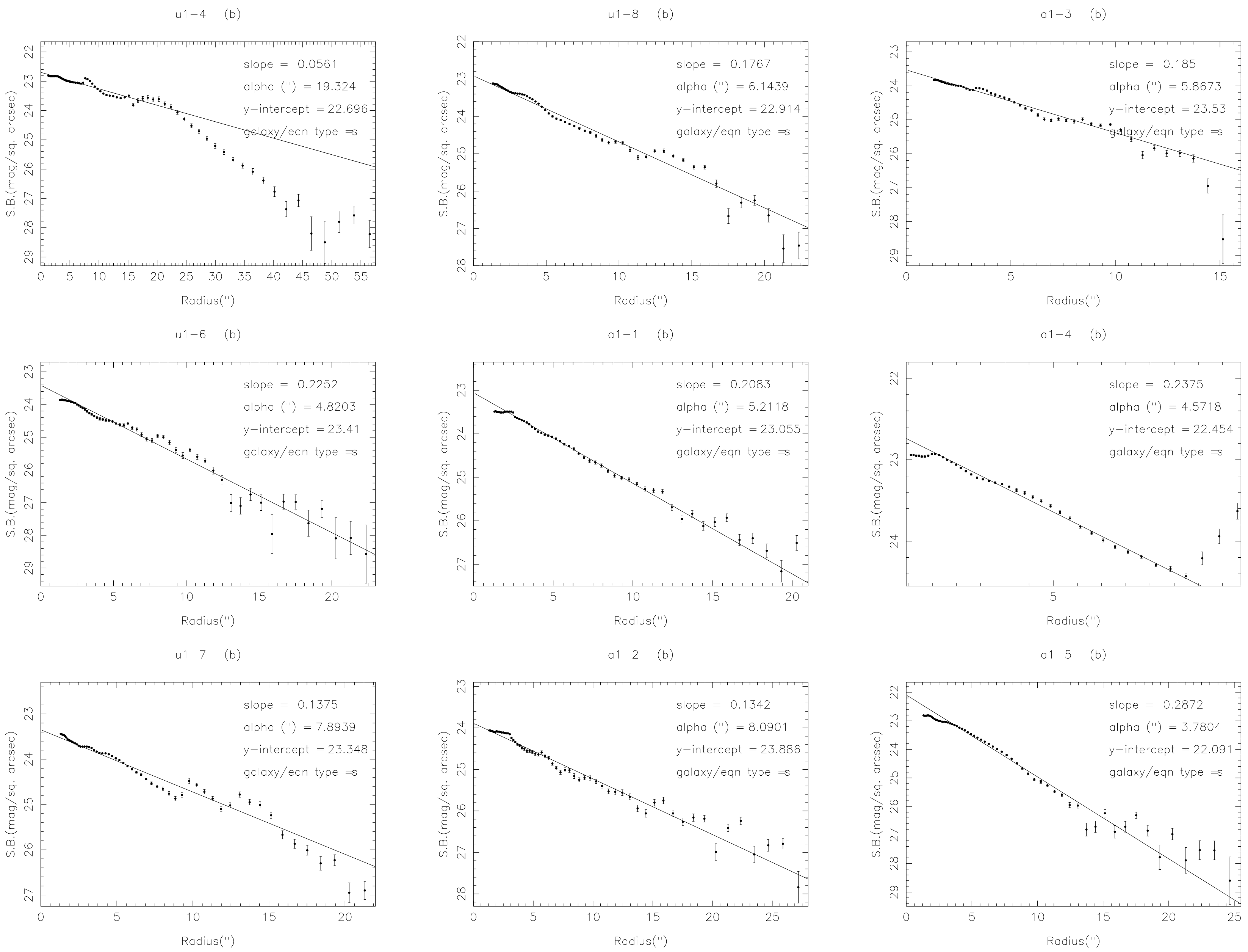
u1-4 (b)
slope = 0.0561
alpha ('') = 19.324
y-intercept = 22.696
galaxy/eqn type =s
u1-8 (b)
slope = 0.1767
alpha ('') = 6.1439
y-intercept = 22.914
galaxy/eqn type =s
a1-3 (b)
slope = 0.185
alpha ('') = 5.8673
y-intercept = 23.53
galaxy/eqn type =s
u1-6 (b)
slope = 0.2252
alpha ('') = 4.8203
y-intercept = 23.41
galaxy/eqn type =s
a1-1 (b)
slope = 0.2083
alpha ('') = 5.2118
y-intercept = 23.055
galaxy/eqn type =s
a1-4 (b)
slope = 0.2375
alpha ('') = 4.5718
y-intercept = 22.454
galaxy/eqn type =s
u1-7 (b)
slope = 0.1375
alpha ('') = 7.8939
y-intercept = 23.348
galaxy/eqn type =s
a1-2 (b)
slope = 0.1342
alpha ('') = 8.0901
y-intercept = 23.886
galaxy/eqn type =s
a1-5 (b)
slope = 0.2872
alpha ('') = 3.7804
y-intercept = 22.091
galaxy/eqn type =s
S.B.(mag/sq. arcsec)
Radius('')

i1-1 (b)

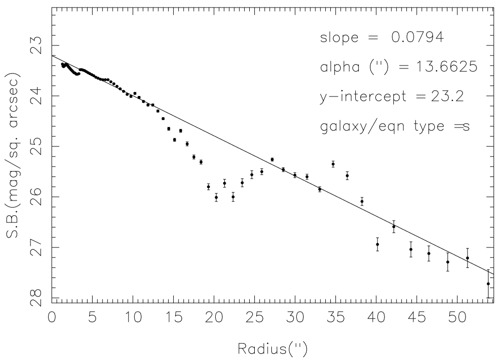

N4-2 (v)

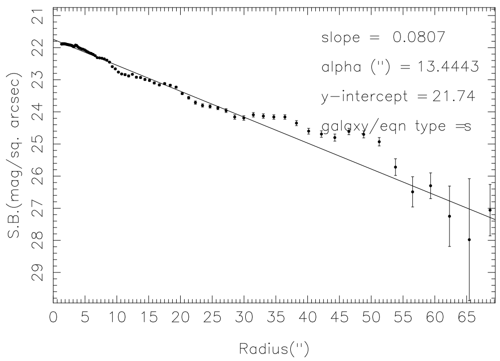

N5-3 (v)

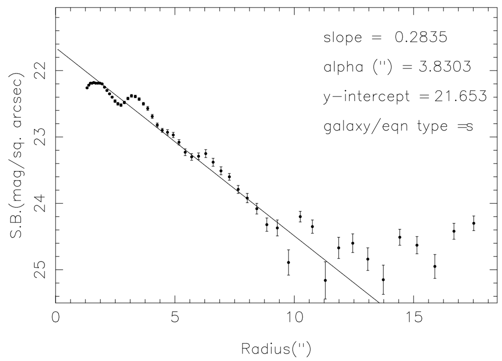

i1-2 (b)

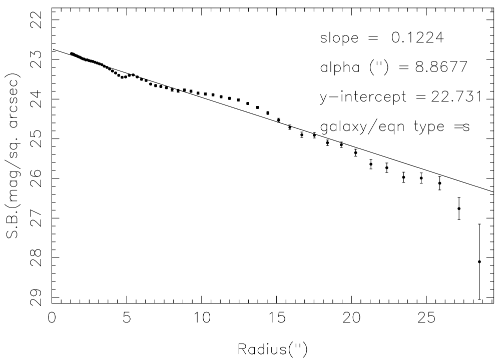

N5-1 (v)

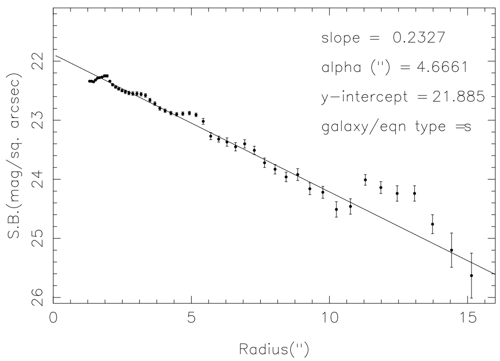

N5-4 (v)

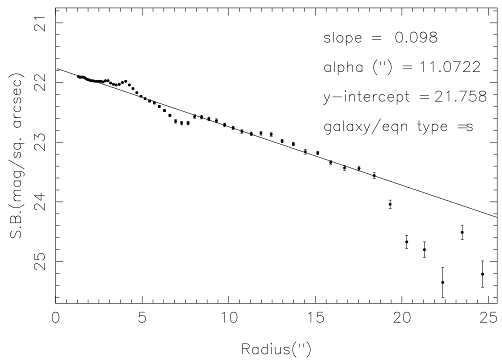

N4-1 (v)

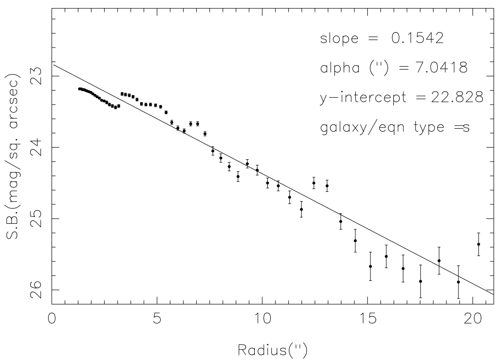

N5-2 (v)

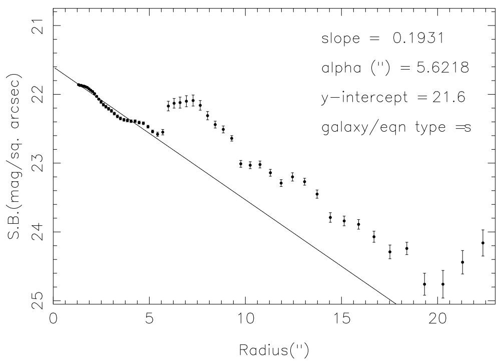

N6-1 (v)

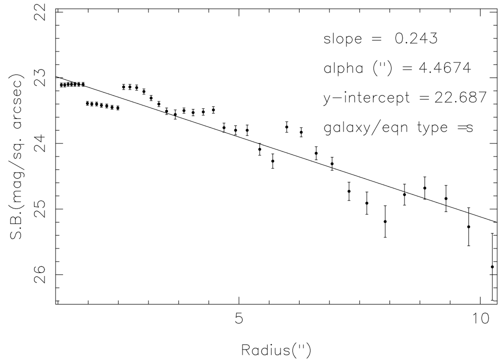

N6-2 (v

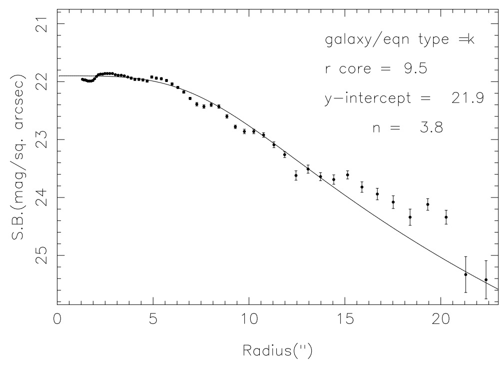

N6-3 (v

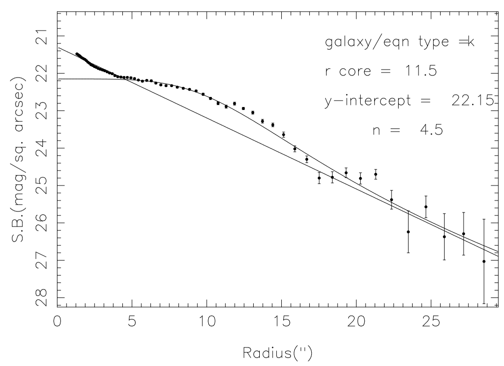

N6-4 (v)